# STUDIES OF SR-BI IN HDL LIPID UPTAKE IN HEPATOCYTES

# STUDIES OF SR-BI IN HDL LIPID UPTAKE IN HEPATOCYTES

By

RACHELLE H. BRUNET, B.SC.

A Thesis

Submitted to the School of Graduate Studies

in Partial Fullfilment of the Requirements

for the Degree

Master of Science

McMaster University

MASTER OF SCIENCE (2007)
(Biochemistry and Biomedical Sciences)

McMaster University
Hamilton, Ontario

TITLE: Studies of SR-BI in HDL Lipid Uptake in Hepatocytes

AUTHOR: Rachelle H. Brunet, B.Sc. (Laurentian University)

SUPERVISOR: Professor Bernardo L. Trigatti

NUMBER OF PAGES: xiv, 94

**Abstract**

Gene-targeted studies in mice have shown that the murine scavenger receptor class B type I (mSR-BI) is atheroprotective and plays a key role in the clearance of high density lipoprotein (HDL) cholesterol by the liver. We focused on the analysis of human SR-BI (hSR-BI) and the role of its C-terminal cytoplasmic tail on its localization, lipid uptake activity, and regulation in hepatocytes both *in vitro* and *in vivo*. Full length hSR-BI and hSR-BI lacking its C-terminal cytoplasmic tail (hSR-BI-DM) localized to vesicle-like structures in the cytoplasm, to juxtanuclear regions and to the cell surface in HepG2 cells. Similar cytoplasmic punctate distribution was observed in transfected human and mouse aortic endothelial cells.

In HepG2 cells both hSR-BI and hSR-BI-DM mediated HDL-lipid uptake; however, the truncation mutant displayed only half of the activity, suggesting that removal of the C-terminal cytoplasmic tail reduced but did not eliminate SR-BI's activity. In HepG2 cells treated with the PKC inhibitor, calphostin C, hSR-BI or hSR-BI-DM mediated HDL-lipid uptake was decreased by 40 and 50%, respectively, indicating that this activity is regulated by PKC.

In order to determine the effects of hSR-BI and hSR-BI-DM *in vivo*, we set out to generate transgenic mice with hepatic overexpression of each protein using a bipartite expression system requiring driver and responder transgenes. Mice expressing the responder transgenes, $P_{TRE}$hSR-BI and $P_{TRE}$hSR-BI-DM, as well as a reporter transgene

($P_{TRE}$lacZ), driven by the same bi-directional promoter, were generated and mated to mice with a liver-specific driver transgene, $P_{MUP}$tTA. The mice were analyzed and showed the presence of a reporter protein, β-galactosidase, in their livers, but not in other tissues tested. Total and HDL cholesterol levels were not altered in $P_{MUP}$tTA / $P_{TRE}$hSR-BI or $P_{MUP}$tTA / $P_{TRE}$hSR-BI-DM transgenic mice. Further characterization of the double transgenic mice revealed that hSR-BI mRNA transcripts were detected in the livers of $P_{MUP}$tTA / $P_{TRE}$hSR-BI mice, but not in those of $P_{MUP}$tTA / $P_{TRE}$hSR-BI-DM mice. However, neither $P_{MUP}$tTA / $P_{TRE}$hSR-BI nor $P_{MUP}$tTA / $P_{TRE}$hSR-BI-DM mice showed increased expression of SR-BI in their livers.

**Acknowledgements**

I extend my utmost gratitude to my supervisor Dr Bernardo Trigatti. Through his patient teachings, I have learned not only a wealth of scientific knowledge, but also the importance of a good work ethic. His enthusiasm and his continual help have been invaluable throughout my graduate studies. I wish him nothing but the greatest success in the future.

I am very appreciative of my committee members, Dr Geoff Werstuck and Dr Suleiman Igdoura, for their encouragement and helpful recommendations.

I am grateful to members of the Trigatti lab with which I had the pleasure to work. In particular, I thank Vivienne for being a helpful scientific resource, but more importantly, a constant source of support and an incredible friend. In addition, I thank Heather Gray for being an entertaining comrade and a genotyping whiz. I am also appreciative of Ayesha Ahmed, Xing Chen, Laney Fiebig, Maxine How, JP King, Dan Kim, Rebecca Pearce, Elizabeth Roediger and Yi Zhang for their help and for providing an enjoyable atmosphere in which to work.

I am also incredibly thankful to my family. My parents, Gilles and Louise Brunet, through the examples they have set, have taught me qualities required not only to succeed, but to be happy in life. Without their constant encouragement and the loving environment they have provided, I would not be where I am today. My siblings, Gilbert, Paul and Roxanne Brunet, have brought out my competitive drive and fierce determination, qualities that were essential in the completion of this task. In addition, I'd like to thank Paul for our "Sunday night dinners", this tradition has meant a lot to me and helped to make me feel close to the whole family.

I am also sincerely grateful to Scott Bindner for his partnership and the moral support he has provided during the most difficult part of my graduate work. His sweet and understanding nature has kept me balanced and has been paramount to my success.

## Table of Contents

## List of Figures

## List of Tables

## List of Abbreviations

| | |
|---|---|
| apo B-100 | apolipoprotein B-100 |
| apo E | apolipoprotein E |
| APMSF | 4-amido-phenyl methane sulfonyl fluoride |
| BCA | bicinchoninic acid |
| BLT-1 | blocker of lipid transport 1 |
| BSA | bovine serum albumin |
| cPBS | complete phosphate buffered saline |
| CE | cholesterol ester |
| CHO | Chinese hamster ovary |
| CMV | cytomegalovirus |
| CUG | carboxy-umbelliferyl β-D-galactopyranoside |
| DAPI | 4',6-diamidino-2-phenylindole |
| dATP | deoxyadenosine triphosphate |
| DIC | differential interference contrast |
| DiI | 1,1'-dioctadecyl-3,3,3',3'-tetramethylindocarbocyanine perchlorate |
| DMEM | Dulbecco's modified Eagle's medium |
| dNTP | deoxynucleoside triphosphate |
| DTT | dithiothreitol |
| EDTA | ethylene dinitrilio tetraacetic acid |
| EGFP | enhanced green fluorescent protein |

| | |
|---|---|
| eNOS | endothelial nitric oxide synthase |
| ERC | endosomal recycling compartment |
| FBS | fetal bovine serum |
| FC | free cholesterol |
| FPLC | fast pressure liquid chromatography |
| HAEC | human aortic endothelial cells |
| HDL | high density lipoprotein |
| HEK | human embryonic kidney |
| HRP | horseradish peroxidase |
| hSR-BI | human scavenger receptor class B type I |
| hSR-BI-DM | human scavenger receptor class B type I C-terminal tail deletion mutant |
| i.p. | intraperitoneal |
| kDa | kilo Dalton |
| IDL | intermediate density lipoprotein |
| LB | Luria Bertani medium |
| LDL | low density lipoprotein |
| LDLR | low density lipoprotein receptor |
| MAEC | murine aortic endothelial cells |
| MDCK | Madin-Darby canine kidney |
| MCP-1 | monocyte chemoattractant protein-1 |
| MRFP | monomeric red fluorescent protein |
| mSR-BI | murine scavenger receptor class B type I |

| | |
|---|---|
| ONPG | o-nitrophenyl-β-D-galactopyranoside |
| PBS | phosphate buffered saline |
| PCR | polymerase chain reaction |
| PEG | polyethylene glycol |
| PI3K | phosphatidyl inositol 3 kinase |
| PKC | protein kinase C |
| PMA | phorbol myristate acetate |
| PVDF | polyvinylidene fluoride |
| RCT | reverse cholesterol transport |
| RT | room temperature |
| SDS | sodium dodecyl sulphate |
| SDS-PAGE | sodium dodecyl sulphate polyacrylamide gel electrophoresis |
| SR-AI | scavenger receptor class A type I |
| SR-AII | scavenger receptor class A type II |
| SR-BI | scavenger receptor class B type I |
| SR-BII | scavenger receptor class B type II |
| TRE | tetracycline responsive element |
| tTA | tetracycline transactivator |
| u | unit |
| VCAM-1 | vascular cell adhesion molecule-1 |
| VLDL | very low density lipoprotein |

# A. Introduction

## A.1. Atherosclerosis

Atherosclerosis is a leading cause of morbidity and mortality in the Western world. The progression of this disease begins early in life and continues through to adulthood where it can lead to stroke, coronary artery disease or peripheral artery disease (Viles-Gonzalez et al. 2004). Several genetic and environmental factors are believed to increase the development of atherosclerosis (Stocker et al. 2004). It is now well established that high serum cholesterol concentrations are an important risk factor (Lamarche et al. 1998). Cholesterol and other lipids are transported through polar environments by complexes called lipoproteins (Parathath et al. 2004). Lipoproteins are composed of a polar shell, made up of phospholipids, cholesterol and apolipoproteins, and a neutral core, consisting of triglycerides and cholesteryl esters (Krieger 1998). They are classified according to their density and their molecular components (Tulenko et al. 2002). Of the various lipoproteins classes, low density lipoprotein, LDL, and high density lipoprotein, HDL, are important in atherosclerosis since LDL, known as the "bad cholesterol", is correlated with the development of atherosclerosis (Brown et al. 1986), while HDL, the "good cholesterol", has been correlated with atheroprotection (Gordon et al. 1989).

## A.2. LDL and Atherosclerotic Plaque Development

LDL has been implicated in the earliest step in the development of atherosclerotic lesions: fatty streak formation (Jessup et al. 2004). In the initial phase of fatty streak

development, LDL accumulates within the intima, the layer of the artery wall which is closest to the lumen and which is composed of endothelial cells, extracellular matrix and proteoglycan (Skalen et al. 2002; Stocker et al. 2004). According to the response-to-retention hypothesis, it is believed that once within the arterial wall, LDL retention is largely due to interactions that occur between matrix molecules, such as proteoglycans, and LDL's apolipoprotein, known as apolipoprotein B-100 (apo B-100) (Skalen et al. 2002). The oxidation hypothesis indicates that following its retention within the intima, LDL is modified through the oxidation of both its lipid and protein components by cells located within the arterial wall, such as endothelial cells, macrophages and smooth muscle cells (Hansson et al. 2002; Jang et al. 2004; Stocker et al. 2004). The oxidation of LDL's lipid components leads to modification of the lysine groups on Apo B-100, increasing the net negative charge of LDL (Williams et al. 1995).

The modified lipid components of LDL, including lysophophatidyl choline and other phospholipids, are believed to be able to trigger the expression of vascular cell adhesion molecule-1 (VCAM-1), a leukocyte adhesion molecule, by endothelial cells (Kume et al. 1992). Once bound to VCAM-1, leukocytes can migrate into the intima due to chemoattractant molecules (Hansson et al. 2002; Libby et al. 2002). Specifically, monocyte migration into the arterial wall at sites of lesions is believed to occur due to a chemokine known as monocyte chemoattractant protein-1 (MCP-1) (Gosling et al. 1999). MCP-1's correlation to atherogenesis was demonstrated experimentally by the protection from atherogenesis and macrophage recruitment in the intima observed in human Apo B

expressing mice lacking the MCP-1 gene (Gosling et al. 1999). Within the intima, monocytes differentiate into macrophages due to macrophage colony stimulating factor, a cytokine expressed by macrophages and vascular cells (Qiao et al. 1997). Macrophages are capable of taking up modified LDL through the mediation of scavenger receptors, such as Scavenger Receptor Class A Types I and II (SR-AI/II) and CD36 (Linton et al. 2003). The cholesteryl esters from the lipoproteins accumulate within macrophages generating lipid laden foam cells, the hallmark of an atherosclerotic plaque (Tulenko et al. 2002).

The further accumulation of foam cells and the necrosis of macrophages lead to an extracellular lipid deposit known as a necrotic core (Stocker et al. 2004). The inflammatory response causes smooth muscle cells to enter the intima, proliferate and produce extracellular matrix, including collagen, leading to the formation of a fibrous cap, a thick separation of the core from the arterial lumen, which causes a reduction of the lumen diameter (Teiger 2001; Stocker et al. 2004). Plaques with small necrotic cores and thick fibrous caps are considered stable, as they are less likely to rupture (Fuster et al. 1992). However, further macrophage necrosis, which causes an increase in the size of the necrotic core, and macrophage production of metalloproteinases, which break down collagen and lead to the thinning of the fibrous cap, can lead to plaque instability. (Hartung et al. 2004). The plaques are then at a higher risk for ruptures which could lead to the formation of thrombi and to myocardial infarctions or strokes (Fuster et al. 1992).

## A.3. HDL and Reverse Cholesterol Transport

Contrarily to LDL, HDL has been implicated in atheroprotective pathways, such as reverse cholesterol transport (RCT) (Glomset 1968; Gordon et al. 1989). RCT is a pathway that involves the efflux of free cholesterol (FC) from peripheral tissues to the surface of newly synthesized HDL particles (Tulenko et al. 2002). HDL can also take up cholesterol through efflux mediated by passive diffusion (Mendez 1997). The cholesterol is then esterified by lecithin cholesteryl acyl transferase (Glomset 1968). The cholesterol esters (CE) may now be transferred to other lipoproteins, including LDL and very low density lipoprotein (VLDL), by cholesteryl ester transfer protein (Tall et al. 2000). Remaining cholesterol can be transferred to the liver, for excretion into bile or to be recycled for use in novel lipoprotein synthesis, or to steroidogenic tissues, for the production of steroid hormones (Rigotti et al. 1997). This transfer occurs via a process known as selective cholesterol uptake (Glass et al. 1983). Selective uptake of lipids from HDL has been shown to be mediated by the scavenger receptor, class B type I (SR-BI) in cells overexpressing this receptor (Acton et al. 1996).

## A.4. Scavenger Receptor Class B Type I

### A.4.1. SR-BI Structure, Expression and Ligands

SR-BI is a member of the CD36 protein family (Krieger 2001). It is a 509 amino acid and 82 KDa protein (Acton et al. 1994). SR-BI has short N and C-terminal cytoplasmic domains situated next to N and C-terminal transmembrane domains and a large, N-glycosylated extracellular loop (Acton et al. 1994; Babitt et al. 1997). This

protein exists in monomeric, dimeric and tetrameric forms (Reaven et al. 2004; Sahoo et al. 2006). Recently, it has been demonstrated using fluorescence resonance energy transfer (FRET) that the C-terminal tails of SR-BI monomers are within 10 nm of one another, supporting the evidence that SR-BI homo-dimerizes (Sahoo, Peng et al.). Since it has previously been shown that SR-BI forms oligomers in the absence of its C-terminal tail, it has been proposed that oligomerization is mediated by the C-terminal transmembrane domain or a portion of the extracellular loop in close proximity to it (Sahoo, Darlington et al.; Sahoo, Peng et al.). SR-BI is expressed in the liver, steroidogenic tissues, macrophages and endothelial cells (Acton et al. 1996). SR-BI is a multiligand receptor, binding to lipoproteins, including HDL (Acton et al. 1996), VLDL (Calvo et al. 1997) and LDL (Acton et al. 1994), modified lipoproteins, such as OxLDL (Gillotte-Taylor et al. 2001) and acetylated LDL (Acton et al. 1994), advanced glycation end products (Ohgami et al. 2001), apolipoproteins (Liadaki et al. 2000; Williams et al. 2000), anionic phospholipids (Rigotti et al. 1995) and apoptotic cells (Murao et al. 1997). Its ability to act as a cell surface receptor for HDL and its ability to bind apolipoproteins on the surface of HDL has been the focus of many studies.

### A.4.2. SR-BI and Cholesterol Metabolism *In Vivo*

Experiments conducted using animal models have been very helpful in the determination of SR-BI's role in HDL metabolism. Mice with attenuated hepatic SR-BI expression and SR-BI knockout mice have increased plasma HDL cholesterol levels (Rigotti et al. 1997; Varban et al. 1998; Huby et al. 2006), while mice with hepatic

overexpression of SR-BI have decreased plasma HDL cholesterol concentrations (Kozarsky et al. 1997; Wang et al. 1998; Ueda et al. 1999). Similarly, decreases in plasma HDL cholesterol levels were seen in a recent study conducted in New Zealand white rabbits overexpressing human SR-BI; however, the lipoprotein profiles of these animals also showed increases in plasma LDL cholesterol concentrations (Tancevski et al. 2005). In addition, mouse models have also aided in determining SR-BI's correlation to the development of atherosclerosis. Studies have shown that atherosclerosis was accelerated in LDL receptor deficient mice with attenuated hepatic SR-BI expression, LDL receptor and SR-BI deficient mice fed a high fat diet, and apoE and SR-BI deficient mice (Trigatti et al. 1999; Huszar et al. 2000; Covey et al. 2003). Also, mice overexpressing SR-BI in hepatic tissues were found to have decreased levels of atherosclerosis (Arai et al. 1999; Kozarsky et al. 2000; Ueda et al. 2000).

### A.4.3. SR-BI Mediated HDL Lipid Uptake

SR-BI mediates the selective uptake of CE and FC from HDL (Acton et al. 1996; Ji et al. 1999; Silver et al. 2001; Brundert et al. 2005; Shetty et al. 2006; Sun et al. 2006). The extracellular loop of mSR-BI and both glutamine residues at positions 402 and 418 within this region are required for activity (Gu et al. 1998; Gu et al. 2000; Connelly et al. 2001). Murine SR-BI mediated selective HDL lipid uptake occurs largely at the cell surface and in an endocytosis-independent manner in a variety of cells types (Nieland et al. 2005; Harder et al. 2006; Sun et al. 2006; Zhang et al. a 2007). In addition, mSR-BI also mediates low-level endocytic uptake of HDL and resecretion or transcytosis of the

lipoprotein particle to the cell surface (Silver et al. 2001; Rhode et al. 2004; Wüstner et al. 2004; Nieland et al. 2005; Pagler et al. 2006). Endocytic uptake of HDL is not inhibited by blocker of lipid transport-1 (BLT-1), an inhibitor of SR-BI mediated selective HDL-lipid uptake which does not block binding of HDL to the receptor (Nieland et al. 2002; Nieland et al. 2005). Hence, mSR-SI mediates both selective and endocytic HDL lipid uptake, but the former plays a more substantial role overall in lipid uptake (Silver et al. 2001; Nieland et al. 2005).

Interestingly, in cells expressing SR-BII, a splice variant of SR-BI with a different C-terminal tail, lipids are more readily internalized through endocytosis of HDL (Eckhardt et al. 2004). SR-BII's C-terminal domain contains a dileucine motif which confers the receptor its endocytic activity and insertion of this motif in the C-terminus of SR-BI at the same position converts SR-BI to a largely endocytic receptor as well (Eckhardt et al. 2004). In addition, *human* SR-BI has recently been shown to mediate HDL lipid uptake primarily through an endocytic mechanism in CHO cells (Zhang et al. b 2007). *Human* SR-BI also mediates selective lipid uptake at low levels in these cells (Zhang et al. b 2007). In order to determine if, like SR-BII, *human* SR-BI's C-terminal tail contains a motif responsible for the receptors endocytic properties, the effects of various mutants were tested (Zhang et al. b 2007). Deletion of the C-terminal tail or Y471F or Y471D point mutations in this domain of hSR-BI did not convert this protein to a selective lipid uptake receptor (Zhang et al. b 2007).

In addition, recent studies have shown that HDL lipid uptake activity may be regulated by phosphatidyl inositol 3 kinase (PI3K) or protein kinase C (PKC) lling cascades. In 3T3-L1 differentiating adipocytes, wortmannin-induced inhibition of PI3K blocks insulin and angiotensin II mediated translocation of SR-BI to the cell surface (Tondu et al. 2004). Insulin and angiotensin II treatments in these cells lead to increased SR-BI mediated lipid uptake; hence, PI3K may regulate lipid uptake activity in adipocytes (Tondu et al. 2004). Also, wortmannin treatment causes decreases in hSR-BI mediated HDL lipid uptake activity in both ldlA7 and HepG2 cells and increases this activity in ldlA7 cells expressing mSR-BI (Shetty et al. 2006; Zhang et al. a 2007; Zhang et al. b 2007). Inhibition of PKC, with RO-31-8220 or 16 hr PMA treatments decrease HDL lipid uptake of mSR-BI in ldlA7 cells and hSR-BI in HepG2 cells, respectively (Witt et al. 2000; Zhang et al. b 2007), while activation of PKC by PMA has the opposite effect (Zhang et al. a 2007).

### A.4.4. SR-BI Localization

In non-polarized cells SR-BI has been shown to localize to cell membranes. For example, full length or C-terminal truncation mutant mSR-BI expressed in CHO cells localize to the cell surface (Eckhardt et al. 2004), mSR-BI expressed in ldlA7 or Y1-BS1 murine adrenal cells localizes to caveolae (Babitt et al. 1997), and hSR-BI expressed in HepG2 cells localizes to lipid rafts (Rhainds et al. 2004). As well, mSR-BI has a punctate cytoplasmic distribution throughout adipocytes, ldlA7 cells and Y1-SB1 cells

(Babitt et al. 1997; Tondu et al. 2004). A similar distribution of hSR-BI is observed in kupffer cells and macrophages (Nakagawa-Toyama et al. 2005).

In polarized cells SR-BI is consistently localized at the cell surface. Murine SR-BI expressed in liver, intestine and Madin-Darby canine kidney (MDCK) cells, as well as hepatic rat SR-BI localize to both apical and basolateral cell surfaces (Ikemoto et al. 2000; Cai et al. 2001; Silver et al. 2001; Sehayek et al. 2003; Burgos et al. 2004; Eckhardt et al. 2004; Harder et al. 2007). Hepatic hSR-BI also localizes to the cell surface; however, no distinction has been made as to whether it localizes to apical surfaces, basolateral surfaces or both (Nakagawa-Toyama et al. 2005). In addition, mSR-BI in primary mouse hepatocyte couplets localizes in the endosomal recycling compartment (ERC) (Silver et al. 2001). Interestingly, the localization of the receptor in WIF-B cells, polarized hybrid cells generated by fusing rat hepatoma and human fiboroblast cells, is regulated by cholesterol depletion or loading, which lead to basolaterol and apical surface distributions, respectively (Ihrke et al. 1993; Harder et al. 2007).

### A.4.5. SR-BI and PDZK1

PDZK1 is a 519 amino acid and 63 kDa adapter protein that contains 4 PDZ domains (Kocher et al. 1998; Silver 2002). SR-BI interacts with PDZK1 through the last three amino acids, Ala-Lys-Leu, of its C-terminal tail (Ikemoto et al. 2000; Silver 2002). Interestingly, PDZK1 knockout mice have increased plasma total cholesterol levels

similar to those of SR-BI knockout mice (Kocher 2003). In addition, PDZK1 knockout mice have no decreases in SR-BI protein levels in steroidogenic tissues, but have 95% and 50% reductions in SR-BI protein in the liver and the small intestine, respectively. As well, overexpression of wild-type SR-BI in the liver of PDZK1 knockout mice led to functional and cell surface localized SR-BI, and returned normal lipoprotein metabolism, despite the PDZK1 deficiency (Yesilaltay et al. 2006). Therefore, PDZK1 is responsible for the stability of SR-BI, but not its function or localization (Yesilaltay et al. 2006).

### A.4.6. SR-BI Mediated Cell Signalling

Recent research has also focused on SR-BI's ability to mediate the activation of various signalling pathways. Studies have shown that the binding of HDL to SR-BI can activate PKC (Grewal et al. 2003) and phosphoinositol 3 kinase (PI3K) (Li et al. 2002; Mineo and Shaul 2003; Mineo, Yuhanna et al. 2003; Cao et al. 2004) signalling pathways, leading to endothelial nitric oxide synthase (eNOS) activation (Yuhanna et al. 2001; Li et al. 2002; Mineo and Shaul 2003; Mineo, Yuhanna et al. 2003) and migration in endothelial cells (Seetharam et al. 2006), as well as to the inhibition and induction of apoptosis in MCF-7 and endothelial cells, respectively (Cao et al. 2004; Li 2005). Interestingly, a blocking antibody for the C-terminus of SR-BI inhibited eNOS activation in endothelial cells (Yuhanna et al. 2001) and a C-terminal truncation mutant of human SR-BI allowed MCF-7 cells to undergo apoptosis (Cao et al. 2004). Also, decreased expression of SR-BI and PDZK1, an adaptor protein which binds to SR-BI's C-terminus, block HDL mediated inhibition of the expression of adhesion molecules, such as VCAM-

1 (Kimura et al. 2006). These studies indicate that the C-terminal tail of SR-BI may be of importance in the receptor's mediation of various signalling pathways.

### A.5. Experiment Rationale

The aforementioned studies conducted to characterize SR-BI have provided valuable information; however, much remains to be learned about this receptor. In particular, investigating the role of the C-terminal cytoplasmic tail of hSR-BI on localization, function and regulation of the protein in hepatocytes could also provide useful information about the receptor. In addition, the expression of full length or C-terminal truncation mutant hSR-BI in mice could allow the determination of the effects of the human form of the protein and the role of its C-terminus on the development of atherosclerosis and on lipoprotein metabolism *in vivo*.

## B. Materials and Methods

### B.1. Materials

All enzymes for recombinant DNA methods and ExGen 500 transfection reagent were purchased from Fermentas (Burlington, ON). GoTaq Green 2x Master Mix, Taq DNA polymerase and pGEM-Teasy vector were from Promega (distributed by Fisher Scientific, Inc., Nepean, ON), while Vent DNA polymerase was from New England Biolabs Ltd. (Pickering, ON). The pBIGN2 vector, generated by the insertion of 2 novel Not I restriction sites into the pBIG vector (Clontech), and pTet-Off (Clontech) were generously provided by Dr Mansour Husain, University of Toronto, Toronto, ON. The $P_{MUP}$tTA mice were generously provided by Dr T. Jake Liang, National Institutes of Health, Charlestown, MA, USA. The pEGFP-hSR-BI and pMRFP-hSR-BI plasmids were generated by Ayesha Ahmed, while the pEGFP-hSR-BI-DM and pMRFP-hSR-BI-DM plasmids were generated by Elizabeth Roediger. The Perfectprep gel cleanup and GeneClean II agarose gel extraction kits were obtained from Eppendorf (distributed by VWR, Mississauga, ON) and Q-BioGene (Carlsbad, CA, USA), respectively. Cell lines were obtained from the following researchers. Human aortic endothelial cells (HAEC) and HepG2 cells were generously provided by Dr Geoff Werstuck, McMaster University, Hamilton, ON. Murine aortic endothelial cells (MAEC) were prepared from aortic ring explants by Dr Xing Chen. Human embryonic kidney (HEK) 293 cells were kindly provided by Dr Ray Truant, McMaster University, Hamilton, ON. Cell culture reagents, *E.* coli DH5α competent cells, SuperScript III reverse transcriptase, 4',6-diamidino-2-phenylindole (DAPI), 1,1'-dioctadecyl-3,3,3',3'-tetramethylindocarbocyanine perchlorate

(DiI) and 3-carboxy-umbelliferyl β-D-galactopyranoside (CUG) were obtained from Invitrogen (Burlington, ON). Medium 200 was obtained from Cascade Biologics (Portland, OR). The HAEC transfection kit (Ca#VPB-1001) was obtained from Amaxa Biosystems (Markham, ON). Fugene 6 transfection reagent and proteinase K were acquired from Roche (Mississauga, ON). Shandon cryomatrix and Infinity cholesterol reagent were obtained from Thermo Scientific (distributed by Fisher Scientific, Inc., Nepean, ON). Free Cholesterol C Standard Solution was obtained from Wako Chemicals (Richmond, VA, USA). Total RNA purification kits were obtained from Norgen Biotek Corp. (Thorold, ON). Antibodies were obtained from the following companies. Rabbit-anti-SR-BI primary antibodies raised against the C-terminus (NB400-101) and the extracellular loop were obtained from Novus Biologicals (distributed by Cedarlane Laboratories Ltd, Hornby, ON) and EMD Biosciences (distributed by VWR, Mississauga, ON), respectively. The rabbit-anti-GFP antibody (ca # 632459) and the mouse-anti-β-actin primary antibody were acquired from Clontech (Mountain View, CA, USA) and MP Biomedicals (Aurora, OH, USA), respectively. The anti-ε-COP primary antibody was generously provided by Monty Krieger, Massachusetts Institute of Technology, Boston, MA, USA. The donkey anti-mouse or rabbit secondary antibodies conjugated to HRP were obtained from Jackson Immunoresearch (distributed by BioCan Scientific, Inc., Etobicoke, ON). Phorbol myristate-acetate (PMA), endothelial cell growth supplement, heparin, poly-D-lysine, chloroquine diphosphate, o-nitrophenyl-β-D-galactopyranoside (ONPG), were tert-amyl alcohol and 2,2,2-tribromoethyl alcohol all obtained from Sigma-Aldrich Co. (St. Louis, MO, USA). Calphostin C was obtained

from EMD Biosciences (distributed by VWR, Mississauga, ON). The BCA assay kit was obtained from Pierce Biotechnology, Inc. (distributed by Fisher Scientific, Inc., Nepean, ON). Western Lightning Enhanced Chemiluminescence Reagent Plus kit was acquired from PerkinElmer Life and Analytical Sciences (Boston, MA, USA).

## B.2. Methods

### B.2.1. Generation of $pP_{TRE}$hSR-BI and $pP_{TRE}$hSR-BI-DM Plasmids

Human SR-BI (hSR-BI) and hSR-BI-DM (human SR-BI lacking the terminal 45 amino acids which make up its C-terminal tail) transgenes were amplified by PCR in 10 μL reactions mixtures containing 2 mM Tris-HCl pH 8.0, 10 mM KCl, 10 μM EDTA, 100 μM DTT, 5% glycerol, 0.05% Tween 20, 0.05% Nonidet P-40, 200 μM each dNTP, 2 mM $MgCl_2$, 2 μM forward primer, 2 μM reverse primer, 0.025 u/μL Taq polymerase, 0.025 u/μL Vent polymerase and 50 ng of hSR-BI transgene containing plasmid DNA. The primers sequences used for each of the reactions are listed in Table 1. The PCR amplification reactions, run on an Eppendorf Mastercycler, consisted of an initial 10 minute denaturation at 95°C, followed by 31 cycles of 90 s at 95°C, 90 s at 65.9°C or 62.3°C, for the full length and deletion mutant amplifications, respectively, and 60 s at 72°C.

PCR products were subjected to 1% agarose gel electrophoresis and bands were cut out and extracted using the Agarose Gel Extraction Kit. Purified DNA was incubated with Taq DNA polymerase (0.05 u/μL) at 72°C for 30 min in 2 mM Tris-HCl pH 8.0 containing 10 mM KCl, 10 μM EDTA, 100 μM DTT, 5% glycerol, 0.05% Tween 20, 0.05% Nonidet P-40, 200 μM dATP. DNA fragments from the above reaction mixture were used directly in ligation reactions with 50 ng pGEM-TEasy vector, consisting of

**Table 1. PCR primers for the amplification of hSR-BI or hSR-BI-DM transgenes**

| Product | Primer Name | PCR Primers (5'-3') |
|---|---|---|
| hSR-BI | fpo1 | AAT ACC ACT GCA ATG GGC TGC TCC GCC AAA G |
| | rpfl | AGG TCT CGT CGA CTA CAG TTT TGC TTC CTG G |
| hSR-BI-DM | fpo1 | AAT ACC ACT GCA ATG GGC TGC TCC GCC AAA G |
| | Rpdm | AGG TCT CGT CGA CTA GAT TTG GCA GAT GAC AGG |

30 mM Tris-HCl (pH 7.8), 10 mM $MgCl_2$, 10 mM DTT, 1 mM ATP, 5% polyethylene glycol (PEG) (MW8000) and 3 Weiss u/μL T4 DNA ligase (RT for 1 hr). *E. coli* DH5α subcloning efficiency competent cells (50 μL) were transformed from 2 μL of the ligation reaction by incubation on ice for 20 min, heat shock at 37°C for 5 min, prior to the addition of 200 μL of LB medium and incubation with agitation at 37°C for 1 hr. Cells were plated on LB-agar containing ampicillin (100μg/mL) and cultured at 37°C. Colonies were picked and plasmid DNA was prepared by large scale plasmid DNA preparations.

Large scale plasmid preparations using an alkaline lysis with SDS protocol, similar to the alkaline lysis with SDS: midipreparation method outlined in Molecular Cloning: A Laboratory Manual (Sambrook et al. 2001), were performed. Standard alkaline lysis of bacteria was performed. DNA was precipitated with isopropanol and dissolved in TE. LiCl was added to a concentration of 2.5 M and the DNA, soluble in this solution was precipitated with isopropanol. DNA was dissolved in TE containing 20 μg/mL RNase A and incubated at RT for 15 min. DNA was precipitated by the addition of PEG and NaCl which gave final concentrations of 13% and 0.8 M, respectively. The DNA was washed with 70% ethanol and dissolved in TE. DNA was extracted once with chloroform, twice with phenol and once more with chloroform. DNA was precipitated with ethanol and dissolved in TE. DNA was quantified by UV absorbance spectrophotometry at 260 nm.

Both the hSR-BI and hSR-BI-DM transgene containing plasmids were digested with 1 u/μg Not I in Buffer O (50 mM Tris-HCl (pH 7.5), 10 mM $MgCl_2$, 100 mM NaCl and 0.1 mg/mL BSA) for 18 hrs at 37°C. DNA was extracted with a 1:1 phenol/chloroform mixture, precipitated with ethanol following standard procedures, and dissolved in water. Recessed 3'-termini were filled in a reaction mixture, containing 50 mM Tris-HCl (pH 7.8), 5 mM $MgCl_2$, 1 mM DTT, 50 μM each dNTP, and 0.2 u/μL Klenow fragment, at 37°C for 10 min. The enzyme was deactivated by heating to 70°C for 10 min and the DNA was precipitated with ethanol. The plasmid DNA was dissolved in water, digested with 1 u/μg Eco31I in Buffer Y (33 mM Tris-acetate (pH 7.9), 10 mM magnesium acetate, 66 mM potassium acetate and 0.1 mg/mL BSA) for 18 hrs at 37°C to generate the appropriate sticky ends on the inserts and with 1 u/μg Bfu I in Buffer Bfu I (50 mM Tris-Acetate (pH 7.9), 15 mM magnesium acetate, 100 mM potassium acetate and 0.1 mg/mL BSA) for 18 hrs at 37°C to cut the pGEM-Teasy backbone into smaller fragments. The digested DNA samples were subjected to 1% low-melt agarose gel electrophoresis, the appropriate bands were excised and the DNA was purified by several extractions with phenol/chloroform, followed by precipitation with ethanol.

To prepare the vector, pBIGN2 was digested with u/μg Pst I in Buffer O for 18 hrs at 37°C. The DNA was extracted with a 1:1 phenol/chloroform mixture, precipitated with ethanol and dissolved in water. The 5'-overhang of the DNA fragment was filled by a 5 min incubation at RT in a reaction mixture consisting of 67 mM Tris-HCl (pH 7.5), 6.6 mM $MgCl_2$, 1mM DTT, 16.8 mM $(NH_4)_2SO_4$, 100 μM each NTP, and 0.05 u/μL T4

DNA polymerase. The enzyme was inactivated by heating to 70°C for 10 min and the DNA precipitated with ethanol. The DNA was dissolved in deionized water and digested with u/μg Sal I in Buffer O for 18 hrs at 37°C. The enzyme was deactivated by heating to 65°C for 15 min. Calf intestinal alkaline phosphatase was added to the reaction mixture to a concentration of 0.02 u/μL and the solution was incubated at 37°C for 30 min. The enzyme was inactivated by heating to 85°C for 15 min. The digested vector was subjected to 1% low-melt agarose gel electrophoresis, the appropriate band was excised and the DNA was purified by a series of phenol/chloroform extractions and precipitated with ethanol.

To ligate the inserts and the pBIGN2 vector, ligations were performed as previously described, except PEG was not included in the reaction mixture. *E coli.* DH5α cells were transformed with DNA from the ligation reactions as described above. The $pP_{TRE}$hSR-BI and $pP_{TRE}$hSR-BI-DM plasmids obtained were sequenced by dideoxy-sequencing performed at Mobix, the McMaster University sequencing laboratory, to verify that no mutations had been introduced into the sequences.

### B.2.2. Cell Culture

#### B.2.2.1. Cell Growth Conditions

HAEC were cultured in Medium 200 supplemented with low serum growth supplement (2% fetal bovine serum (FBS), 1 μg/mL hydrocortisone, 10 ng/mL human epidermal growth factor, 3 ng/mL basic fibroblast growth factor and 10 μg/mL heparin).

Wild-type and SR-BI deficient MAEC, prepared from aortic ring explants by Dr Xing Chen, were cultured in 40% Ham's F12 medium, 40% Dulbecco's Modified Eagle's Medium (DMEM) and 20% FBS supplemented with 30 μg/mL endothelial cell growth supplement and 10 iu/mL heparin. HepG2 cells were cultured in DMEM containing 5% FBS. ldlA7 (LDL receptor deficient CHO cells), ldlA[mSR-BI] (ldlA7 cells stably overexpressing murine SR-BI) and ldlA[hSR-BI] (ldlA7 cells stably overexpressing human SR-BI) were cultured in Ham's F12 medium containing 5% FBS. HEK 293 cells were cultured in α-Modified Eagle's Medium containing 5% FBS. 3T3-L1 cells were cultured in DMEM containing 10% calf serum. HepG2, ldlA7, ldlA[mSR-BI], ldlA[hSR-BI], HEK 293 and 3T3-L1 growth media were all supplemented with 50 units/mL penicillin, 50 μg/mL streptomycin and 2 mM L-glutamine.

#### B.2.2.2. Cell Propagation

To propagate HAEC, MAEC, HepG2, ldlA7, ldlA[mSR-BI], ldlA[hSR-BI], 3T3-L1 and HEK 293 cells growing in 100 mm dishes, cells were washed twice with 5 mL of 37°C phosphate buffered saline (PBS). For all cell types, excluding HEK 293 cells, cells were incubated in 1 mL of 37°C trypsin-EDTA (0.05% trypsin, 0.53mM EDTA in PBS) for 0.5-3 min, dislodged from the dishes by gentle agitation and 9 mL of growth media warmed to 37°C was added to the dishes to inactivate the trypsin-EDTA solution. For HEK 293 cells, 10 mL of growth media warmed to 37°C was added to the dishes and the cells were removed by gently pipetting the medium onto the surface of the dish.

**B.2.3. Cell Transfection**

HAEC and MAEC were transfected by eletroporation using an Amaxa Nucleofector or a BioRad Gene Pulser II, respectively. HepG2 cells were transfected using Fugene 6 transfection reagent and 3T3-L1 cells were transfected using ExGen 500 transfection reagent. HEK 293 cells were transfected using calcium phosphate mediated transfection. Brief protocols follow.

HAEC's ($5x10^5$) were suspended in 100 µL of RT HAEC Electroporation Buffer, provided with the HAEC Transfection kit. Plasmid DNA (2.5 µg) was added to the cell suspension and the cells were electroporated using the S-05 program using a nucleofector (Amaxa Biosystems). MAEC were released from a 70-80% confluent 100 mm dish as described above and pelleted centrifugation at 500 x *g* for 5 min. Cells were resuspended in 400 µL of RT DMEM, lacking serum and antibiotics. Plasmid DNA (5.0 µg) was added and cells were electroporated in a 0.4 cm cuvette at 200 V and a capacitance of 840-860 µF. Electroporated HAEC and MAEC were plated on 35 mm poly-D-lysine coated, glass-bottomed dishes containing 2 mL of growth medium and cultured for 20-24 hrs prior to use in experiments.

HepG2 cells were seeded at a density of $5x10^5$ cells per well in 6-well dishes. On the following day, 3 µL of Fugene 6 transfection reagent and 97 µL of serum-free DMEM were mixed and incubated at RT for 5 min prior to the addition of 1 µg of plasmid DNA and further gentle mixing. After incubation for a further 20 min the

mixture was added to one well containing 2 mL of fresh growth medium. The dishes were rocked back and forth and side to side to ensure even distribution of the transfection solution. The cells were cultured for 48 hrs prior to use for experiments.

The 3T3-L1 cells were seeded $2x10^4$ cells per dish in 100 mm dishes. The following day, plasmid DNA (14 μg) was diluted in 500 μL of 150 mM NaCl mixed by gentle vortexing and spun down for 5 s in a microfuge. ExGen 500 transfection reagent (46 μL) was added and immediately afterwards, the tube was gently mixed for 10 s. The solution was incubated at RT for 10 min and the entire contents of the tube were added to one 100 mm dish of cells containing 9 mL of fresh growth medium. After 8 hrs, the medium was removed and replaced with fresh growth media. The cells were cultured for an additional 16-40 hrs prior to use in experiments.

The transfection of HEK 293 cells using calcium phosphate was performed according to the protocol outlined in Molecular Cloning: A Laboratory Manual. HEK 293 cells were seeded in a 60 mm dish. The following day, 1 hr prior to transfection, the cells were given fresh growth media. Six μg of plasmid DNA were diluted in 250 μL of 0.1x TE containing 250 mM $CaCl_2$. This solution was mixed with 250 μL 2x Hepes buffered saline (140 mM NaCl, 1.5 mM $Na_2HPO_4$ and 50 mM Hepes), and incubated at RT for 1 min. The solution was added to the dish and immediately distributed by gently rocking the dish. Immediately following the addition of the calcium phosphate-DNA coprecipitate, chloroquine diphosphate was added to the dish to a final concentration of

100μM. Media was replaced with fresh growth media after 5 hrs of incubation at 37°C. The cells were cultured for an additional 40-48 hrs prior to use in experiments.

### B.2.4. Generation of Stable Cells Lines

HepG2 cells were cultured in growth medium containing 500 μg/mL of G418 24 hrs after transfection to select for cells containing the plasmid of interest. After 4 d, cells selected with G418 were also sorted individually into wells of a 96-well plate in order to isolate clonal cell lines. The sorting was performed by Nicole McFarlane in the McMaster University Biophotonics Facility using a Beckman Ultra cell sorter. After sorting, cells were cultured in growth medium containing 500 μg/mL of G418. The medium was replaced with fresh medium every 2 d. Once the cells could be seen in each well, eGFP expression was analyzed by fluorescent wide-field microscopy using an Axiovert 200M inverted fluorescent microscope (Carl Zeiss). Isolates expressing eGFP were expanded and eGFP and SR-BI expression were characterized by immunoblotting and fluorescence microscopy.

### B.2.5. Generation of Transgenic Mice

The $pP_{TRE}$hSR-BI and $pP_{TRE}$hSR-BI-DM plasmids were digested with 1 u/μg Not I in Buffer O for 18 hrs at 37°C to remove bacterial sequences. The $pP_{TRE}$hSR-BI DNA sample was sent to the London Transgenic and Gene Targeting Facility where it was purified and used to generate transgenic mice by pronuclear injections of C57Bl6/CBA F1 hybrid oocytes and reimplantation into pseudopregnant foster mothers. The

$pP_{TRE}$hSR-BI-DM DNA sample was subjected to 1% agarose gel electrophoresis. The band of interest was excised from the gel and the DNA was purified using the GeneClean II Kit following the manufacturer's instructions. DNA was quantified by UV absorbance spectrophotometry at 260 nm and diluted to a concentration of 2 ng/μL in injection buffer (7.5 mM Tris-HCl (pH 7.4) containing 150 μM EDTA). The DNA sample was used by Aline Fiebig in Dr Suleiman Igdoura's laboratory at McMaster University to generate transgenic mice by pronuclear injection of FVB oocytes and reimplantation into pseudopregnant foster mothers.

### B.2.6. Mouse Genotyping

#### B.2.6.1. Genomic DNA Isolation from Mouse Tails

The mice were anaesthetized with 0.2 mL intraperitoneal (i.p.) injections of Avertin (3.54 M 2,2,2-tribromoethyl alcohol in tert-amyl alcohol) (2.5% in PBS). One cm of each tail was removed using a clean razor blade. The wounds were closed using VetBond and the animals were allowed to recover. The tail biopsies were digested in 500 μL of 100 mM Tris-HCl (pH 8.5), 5 mM EDTA, 0.2% SDS, 200 mM NaCl containing 100 μg/mL proteinase K (55°C overnight). Debris was pelleted by centrifugation at maximum speed for 15 min (RT). DNA was precipitated by the addition of 500 μL isopropanol. Using bent pipet tips, the DNA precipitates were removed from the solutions and transferred to microfuge tubes containing 200 μL TE (100 mM Tris-HCl (pH 8.0) and 10 mM EDTA). The tubes were incubated at 37°C overnight to dissolve the

DNA. DNA samples were diluted 1:100 in water and 5 μL was used as template for PCR reactions.

### B.2.6.2. Genotyping PCR

PCR genotyping was done in 25 μL reactions using GoTaq Green PCR Master Mix (Promega) which contains a proprietary buffer (pH 8.5), which includes 1.5 mM $MgCl_2$, 200 μM each dNTP and 25 u/mL Taq DNA polymerase, to which was added 800 nM each forward and reverse primers and 5 μL of tail genomic DNA. The primer sequences, annealing temperatures and amplicon sizes used for each of the three reactions are listed in Table 2. The PCR amplification reactions, run on an Eppendorf Mastercycler, consisted of an initial 2 minute denaturation step at 94°C and a 2 minute annealing step (Table 2). These were followed by 41 cycles of 90 s at 94°C, 90 s at annealing temperatures (Table 2) and 2 min at 72°C. The PCR reaction mixtures were subjected to eletrophoresis on a 0.8% agarose gel containing 5 μg/mL ethidium bromide, and were visualized using a Kodak Imaging Station.

**Table 2. PCR primers to characterize inserted transgenes**

| Product | Primer Name | PCR Primers (5'-3') | Annealing Temperature (°C) | Amplicon (bp) |
|---|---|---|---|---|
| Insert | P1 | TCA CTG CAT TCT AGT TGT GGT | 60.5 | 2393[a], 2258[b] |
| | P4 | GAT GTG CTG CAA GCC GAT | | |
| lacZ 1 | PZ1A | GCT CGT TTA GTG AAC CGT CAG | 64.2 | 2893 |
| | Bgalrev | TAA TCC GAG CCA GTT TAC CC | | |
| lacZ 2 | Bgalfor | ACC GGA TTG ATG GTA GTG GT | 59.1 | 776 |
| | P7 | TGA AGT TCT CAG TCT AGA GTC | | |

### B.2.7. Mouse Tissue Harvesting

Ten week old mice were fasted as of 6 pm the day prior to harvesting. On the day of harvest, mice were anesthetized with Avertin (0.4 mL i.p.). Blood was collected into a heparinized syringe by cardiac puncture. The vasculature was perfused by gravity with ice-cold PBS containing 5 mM EDTA by allowing the buffer to flow in through the left ventricle and out by a cut made in the right atrium. After the perfusion, the liver was harvested first and prepared in the following manner. Two 20 mg pieces were immediately frozen in liquid nitrogen and stored at -80°C for future RNA preparations. Several thin sections were cut with a razor blade, placed in tissue embedding molds containing Shandon Cryomatrix, frozen on dry ice sitting in isopentane, and stored at -80°C. The remaining portions of the livers were cut into two pieces, frozen in liquid nitrogen, and stored at -80°C. The intestines and stomach were cut open using a razor blade, cleaned out, rinsed in PBS containing 5 mM EDTA and frozen in liquid nitrogen and stored at -80°C. All other tissues harvested, including adipose tissue, adrenal glands, brain, heart, kidneys, lungs, skeletal muscle and spleen were directly frozen in liquid nitrogen and stored at -80°C.

### B.2.8. Plasma Lipoprotein Analysis

Blood collected from mice fasted overnight was centrifuged at 12000 x *g* for 5 min. The plasma samples (supernatant) were transferred to fresh tubes and centrifuged a second time at 12000 x *g* for 5 min. The plasma samples were transferred to fresh tubes

and either used immediately or stored at 4 °C. Plasma (100 μL) was fractionated on a Tricorn Superose 6 10/30 GL gel filtration column (GE Healthcare) with 154 mM NaCl /1mM EDTA (pH 8.0) as the elution buffer using an AKTA fast pressure liquid chromatography (FPLC) (flow rate was 0.5 mL/min). Forty-seven 250 μL fractions were collected from the end of the void volume (6.5 mL) to ¾ of the total column volume. HDL and LDL samples prepared from human plasma were also fractionated as described and were shown to elute from the column in this volume (data not shown). In addition, experiments have demonstrated that the major classes of lipoproteins (VLDL, IDL/LDL and HDL) elute within this range (Covey et al. 2003).

The cholesterol concentrations of samples were determined using a colorimetric coupled enzymatic assay consisting of 100 uL of the FPLC fractions or mouse plasma diluted 1:100 and 200 uL of Infinity Cholesterol reagent incubated in 96-well dishes at 37°C for 30 min. Absorbance (500 nm) was measured using a spectrophotometric plate reader. Dilutions of Free Cholesterol C Standard Solution were used to generate the standard curves.

### B.2.9. Reverse-transcriptase PCR

#### B.2.9.1. RNA Preparation

RNA was prepared from 20 mg mouse liver samples using a total RNA purification kit according to the manufacturer's instructions except that tissues were

homogenized by passage through a 30g needle until no visible tissue pieces remained. RNA was quantified by UV absorbance spectrophotometry at 280 nm.

### B.2.9.2. cDNA Synthesis

Solutions consisting of 3.5 mM oligo$(dT)_{20}$, 1.4 mM each dNTP, and 1 μg RNA were heated to 65°C for 5 min then incubated on ice for 1 minute prior to the addition of reaction buffer and reverse transcriptase. Final reaction mixtures consisted of 2.5 mM oligo$(dT)_{20}$, 1 mM each dNTP, 50 mM DTT, 50mM Tris-HCl (pH 8.3), 75 mM KCl, 3 mM $MgCl_2$, 1 μg RNA and 40 u/μL SuperScript III reverse transcriptase in 20 μL. Reactions were carried out at 50°C for 2 hrs and were terminated by heating to 70°C for 5 min. The samples were stored at -20°C.

### B.2.9.3. PCR Amplification

The PCR was performed as outlined for the genotyping PCR, except that 1 μL of a 1 in 5 dilution of cDNA was used as the template and the reactions consisted of an 2 min at 50°C and 10 min at 95°C, followed by 25 cycles of 15 s at 95°C and 60 s at 60°C. The primer sequences used for both the human SR-BI and the murine β-actin reactions are listed in Table 3. The PCR reaction mixtures were run out on a 1.5% agarose gel containing 5 μg/mL ethidium bromide, and were visualized using a Kodak Imaging Station.

**Table 3. Reverse-transcription PCR primers**

| Product | Primer Name | PCR Primers (5'-3') | Amplicon (bp) |
|---|---|---|---|
| Human SR-BI | hSR-BIFor | GTA CAG GGA GTT CAG GCA CA | 85 |
| | hSR-BIRev | GAA CTG GAA GGT GCG GTA CT | |
| Murine β-actin | mbactinFor | ACC AAC TGG GAC GAT ATG GAG AAG A | 250 |
| | mbactinRev | TAC GAC CAG AGG CAT ACA GGG ACA A | |

### B.2.10. Preparation of Cellular Homogenates

Frozen tissue samples were thawed on ice. Lysis buffer, comprised of 0.2 x PBS containing 0.1% Triton X-100, 100 μM 4-amido-phenyl methane sulfonyl fluoride (APMSF), 2 μM leupeptin, 300 nM aprotinin and 1.5 μM pepstatin A, was added (1.5 mL/g of tissue). The tissues, with the exception of adrenal glands and spleens, were homogenized in a glass tube with a Teflon pestle for 3 min with several upward and downward strokes. The adrenal glands and spleens were homogenized by continuous sonication for 15-30 s using a Cell Disrupter 350 (Sonifer) set at a 40% duty cycle and at an output of 4. The homogenates were transferred to microfuge tubes and subjected to centrifugation at 4°C and 12000 rpm for 15 min to pellet the nuclei and cell debris. The supernatants were removed and transferred to fresh tubes. The lysates were used immediately for β-galactosidase assays. Aliquots were flash frozen in liquid nitrogen and stored at -80°C for further analysis such as immunoblotting for SR-BI and β-galactosidase.

### B.2.11. β-galactosidase Assay

Cell lysates and mouse tissue homogenates were assayed in 96-well plates, in reaction mixtures consisting of 0.1 M sodium phosphate (pH 7.3), 1 mM $MgCl_2$, 45 mM β-mercaptoethanol and 3 mM ONPG or 0.1 mM CUG, respectively. When ONPG was used as the substrate, 75 μL reaction mixtures were incubated at 37 °C for 45 min, 125 μL of 1 M $Na_2CO_3$ was added to each sample and the absorbance was measured at 420 nm using a spectrophotometric plate reader. When CUG was used as a substrate, 110 μL

reaction mixtures were protected from light and incubated at RT for 30 min. 50 µL of 0.2 M $Na_2CO_3$ was added to each sample and the plate was read in an Applied Biosystems CytoFluor Series 4000 fluorescence plate reader set at an excitation filter of 360/40 nm, an emission filter of 460/40 nm and a gain of 40. Protein concentrations were also determined and used to determine the specific β-galactosidase activity of the samples.

### B.2.12. Protein Assay

The protein concentrations of cell lysates were determined using bovine serum albumin as a standard and a bicinchoninic acid (BCA) assay kit for which the absorbance was measured at 562 nm.

### B.2.13. SDS-PAGE Electrophoresis

SDS-PAGE was performed according to the methods outlined by Laemmli (Laemmli 1970) using tissue homogenates, prepared as described above, or cell lysates, prepared by lysis in 0.2 x PBS containing 0.1% Triton X-100, 100 µM APMSF, 2 µM leupeptin, 300 nM aprotinin and 1.5 µM pepstatin A. SDS-PAGE was carried out using polyacrylamide gels consiting of both stacking gels (125 mM Tris-HCl pH 6.8, 0.1 % SDS, 5% acrylamide (40:1 acrylamide to bisacrylamide) and separating gels (375 mM Tris-HCl pH 8.8, 0.1% SDS, 8, 10 or 15 % acrylamide (40:1 acrylamide to bisacrylamide). Prior to loading, samples were solubilized in 3 x loading buffer (150mM Tris-HCl pH 6.8, 6% SDS, 0.3% bromophenol blue, 30% glycerol and 40 mM DTT) by

heating at 95°C for 5 min. The samples were electrophoresed at 200 V in 192 mM glycine, 25 mM Tris and 1% SDS for 40-60 min.

### B.2.14. Electrophoretic Transfer

Electrophorectic transfer was performed as outlined by Towbin et al. 1979. The polyacrylamide gels obtained after SDS-PAGE were incubated in transfer buffer (192 mM glycine, 25 mM Tris and 20% methanol) for 15 min. Polyvinylidene fluoride (PVDF) membrane was incubated in methanol for 30 s, washed 3 times in deionized water and also incubated in transfer buffer for 15 min. Following the incubations, the proteins separated out on the polyacrylamide gels were transferred onto the PVDF membrane by electrophoresis on ice. Electrophoresis was performed using either a BioRad Mini Trans-Blot apparatus at 50 V for 40 min or an Idea Scientific transfer apparatus at 12 V for 1 hr.

### B.2.15. Immunoblotting

The PVDF membranes obtained after the protein transfer were blocked by incubation with 5% skim milk in PBS with 0.1% Tween-20 (PBST) with agitation at RT. The blots were incubated with primary antibody by rocking for 1 hr at RT. The blots were washed 3 times with PBST for 15 minute by rocking at RT and incubated with a secondary antibody by rocking for 1 hr at RT. The blots were washed twice for 15 min with PBST and once for 15 min with PBS with rocking at RT. The blots were incubated for 1 minute in Western Lightning Enhanced Chemiluminescence Reagent Plus kit and

were then exposed to x-ray film (X-blue, Kodak). The rabbit anti-SR-BI primary antibodies recognizing either the C-terminal tail or the extracellular loop and the rabbit anti-GFP polyclonal primary antibody were used at 1:1000 dilutions in PBST. The mouse anti-β-galactosidase, the rabbit anti-ε-COP and the mouse anti-β-actin primary antibodies were used at 1:2000, 1:5000 and 1:30000 dilutions in PBST, respectively. Donkey anti-rabbit or mouse secondary antibodies conjugated to horseradish peroxidase were used at dilutions of 1:10000 in PBST.

### B.2.16. Fluorescence Microscopy

Cells cultured on poly-D-lysine coated, glass-bottomed dishes were fixed with freshly prepared 2.5% paraformaldehyde in PBS. Cells were incubated for 4 min in 2 mL of 300 nM DAPI in PBS to stain nuclei. Stained cells were washed 3 times with PBS, and fluorescence microscopy was performed using an Axiovert 200M inverted fluorescence microscope (Carl Zeiss). Fluorescence images were captured with either Fs01 (excitation: band pass 365/12 and emission: long pass 397), Fs10 (excitation: band pass 450-490 and emission: band pass 515-565), Fs13 (excitation: band pass 470/20 and emission: band pass 505-530) and Fs15 (excitation: band pass 546/12 and emission: long pass 590) Zeiss filter sets. Differential interference contrast (DIC) images were also captured. The contrast of each fluorescent image was adjusted linearly using Adobe Photoshop Elements. The red, green and blue channels were adjusted independently.

**B.2.17. DiI-HDL Lipid Uptake Assay**

HDL was prepared from human plasma by KBr ultracentrifugation and labelled with DiI as previously described (Chapman et al. 1981; Reynolds et al. 1985; Acton et al. 1996). On day 0, 500 000 HepG2 cells were seeded per well of 6-well dishes. On day 2, the cells were washed once with 1 mL of incomplete DMEM. For experiments requiring the treatment of cells with various inhibitors or activators, the cells were incubated in incomplete DMEM containing 0.5% BSA and the inhibitor or activator at the appropriate concentration for 10 min at 37°C.

Following these incubations, DiI-HDL was added to each well to a final concentration of 5 μg/mL and cold HDL was added to one half of the wells from each of the various treatments at a final concentration of 200 μg/mL. For experiments without treatments with inhibitors or activators, the DiI-HDL and cold HDL were added immediately after the wash with incomplete DMEM at the final concentrations stated above. The plates were incubated at 37°C for 2 hrs. The cells were washed twice with cPBS (PBS containing 0.01% $CaCl_2$ and 0.01% $MgCl_2$) and visualized using a Zeiss Axiovert 200M inverted fluorescence microscope and Fs15 (excitation: band pass 546/12 and emission: long pass 590) Zeiss filter set to verify the presence of red fluorescence in the cells. The cells were released from the dishes by trypsinization (0.05% trypsin, 0.53mM EDTA in PBS) for 2 min. One mL of ice-cold complete media was added to each well of cells and the cell suspensions were transferred to 12 x 75 mm tubes. The cells were pelleted at 500 x *g* for 15 min. The supernatants were removed and the cells

were resuspended in ice-cold PBS containing 0.1% BSA, 0.5 mM EDTA and 0.1% glucose.

The samples were analyzed for DiI and eGFP fluorescence using a Beckman Coulter Epics XL flow cytometer by Nicole McFarlane in the laboratory of Douglas Boreham at McMaster University. For cells HepG2 cells stably transfected with eGFP-hSR-BI and eGFP-hSR-BI-DM, the mean DiI fluorescence of eGFP positive cells only was used in the analysis of the data. The DiI-HDL lipid specific uptake of samples was determined by subtracting the mean DiI fluorescence of the cells treated with DiI-HDL and cold HDL competitor from that of the cells treated with DiI-HDL only.

# C. Results

## C.1. Investigation of the Role of the C-terminal Cytoplasmic Tail of hSR-BI on the Localization, Activity and Regulation of the Protein

### C.1.1. Localization of hSR-BI and hSR-BI-DM in HAEC, MAEC and HepG2 cells

Recently, several studies have focused on SR-BI's C-terminal cytoplasmic tail. Research has shown that SR-BI mediates activation of PI3K and PKC cell signalling pathways (Li et al. 2002; Grewal et al. 2003; Mineo and Shaul 2003; Mineo, Yuhanna et al. 2003; Cao et al. 2004) and downstream processes, such as migration, eNOS activation and the prevention of apoptosis in endothelial cells (Yuhanna et al. 2001; Li et al. 2002; Mineo and Shaul 2003; Mineo, Yuhanna et al. 2003; Li 2005; Seetharam et al. 2006). However, eNOS activation was inhibited by an SR-BI blocking antibody which binds to the C-terminus of SR-BI (Yuhanna et al. 2001). In addition, decreased expression of SR-BI or its adaptor protein, PDZK1, block the inhibition of the expression of adhesion molecules, such as VCAM-1, mediated by HDL (Kimura et al. 2006).

In addition, hepatic SR-BI mediates selective lipid uptake from HDL (Ji et al. 1999; Brundert et al. 2005; Sun et al. 2006) and plays an important role in atheroprotection and cholesterol metabolism in mice (Kozarsky et al. 1997; Varban et al. 1998; Wang et al. 1998; Arai et al. 1999; Ueda et al. 1999; Huszar et al. 2000; Kozarsky et al. 2000; Ueda et al. 2000; Huby et al. 2006). However, the role of SR-BI's C-terminal tail in hepatocytes has not been fully characterized. In view of this information, we were

interested in further characterizing the role of the C-terminal tail of SR-BI on the protein's localization, function and regulation in endothelial cells and hepatocytes.

The localization of both full length and C-terminal truncation mutant hSR-BI in HAEC and MAEC was determined using hSR-BI full length and C-terminal tail truncation mutant proteins, tagged with EGFP at their amino termini (Fig 1). EGFP-hSR-BI and EGFP-hSR-BI-DM proteins were previously characterized in ldlA7 cells and shown to have HDL-lipid uptake activity (Zhang et al. b 2007). Cells were transfected with EGFP-hSR-BI or EGFP-hSR-BI-DM by electroporation and imaged by fluorescence microscopy (refer to B.2. Methods). Representative images show that in HAEC (Fig 2) and WT or SR-BI-null MAEC (Fig 3) both EGFP-tagged hSR-BI and hSR-BI-DM were distributed in a punctate pattern within cells suggesting that they might associate with vesicles in the cytoplasm. In addition, these results indicate that deletion of the C-terminal tail of SR-BI does not affect the proteins localization in primary human or murine aortic endothelial cells.

The localization of EGFP-tagged or MRFP-tagged full length or C-terminal truncation mutant human SR-BI in HepG2 cells was also determined. HepG2 cells were transfected with each of the constructs independently using Fugene 6 transfection reagent (Roche) and imaged by fluorescence microscopy (refer to B.2. Methods). All 4 fluorescently-tagged proteins localized to juxtanuclear regions, punctate patterns within cells and to the cell periphery (Fig 4). In addition, in a small proportion of cells,

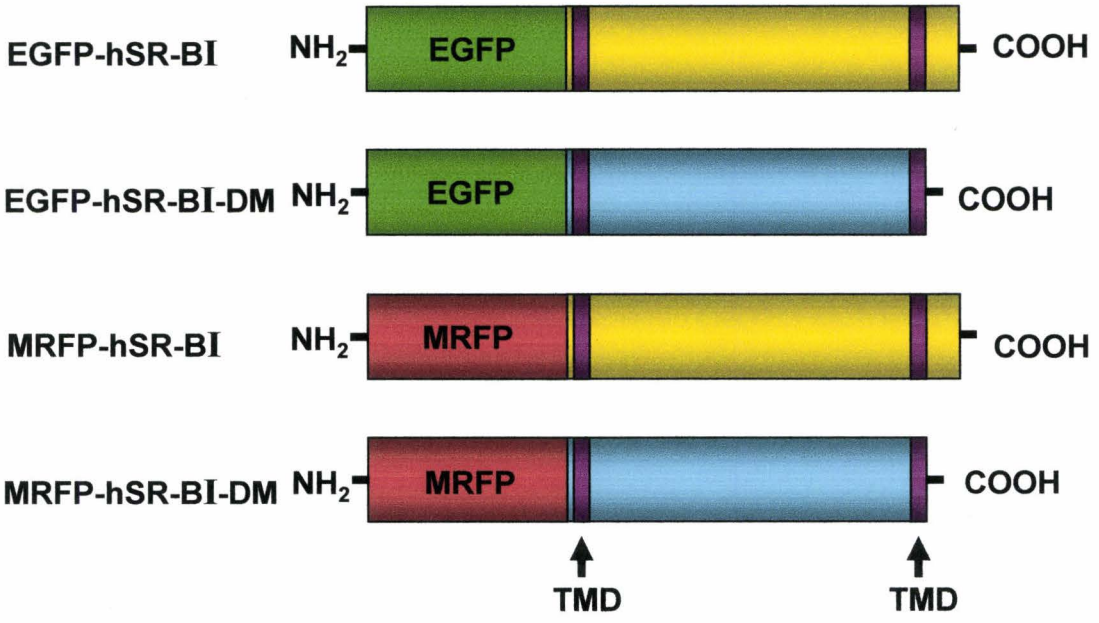


**Figure 1. Diagrams of the EGFP or MRPF-tagged hSR-BI and of the EGFP or MRFP-tagged hSR-BI-DM transgenes.** The constructs consist of either hSR-BI or hSR-BI-DM tagged with either EGFP or MRFP on their amino termini. The location of putative transmembrane domains (TMD) are also shown.

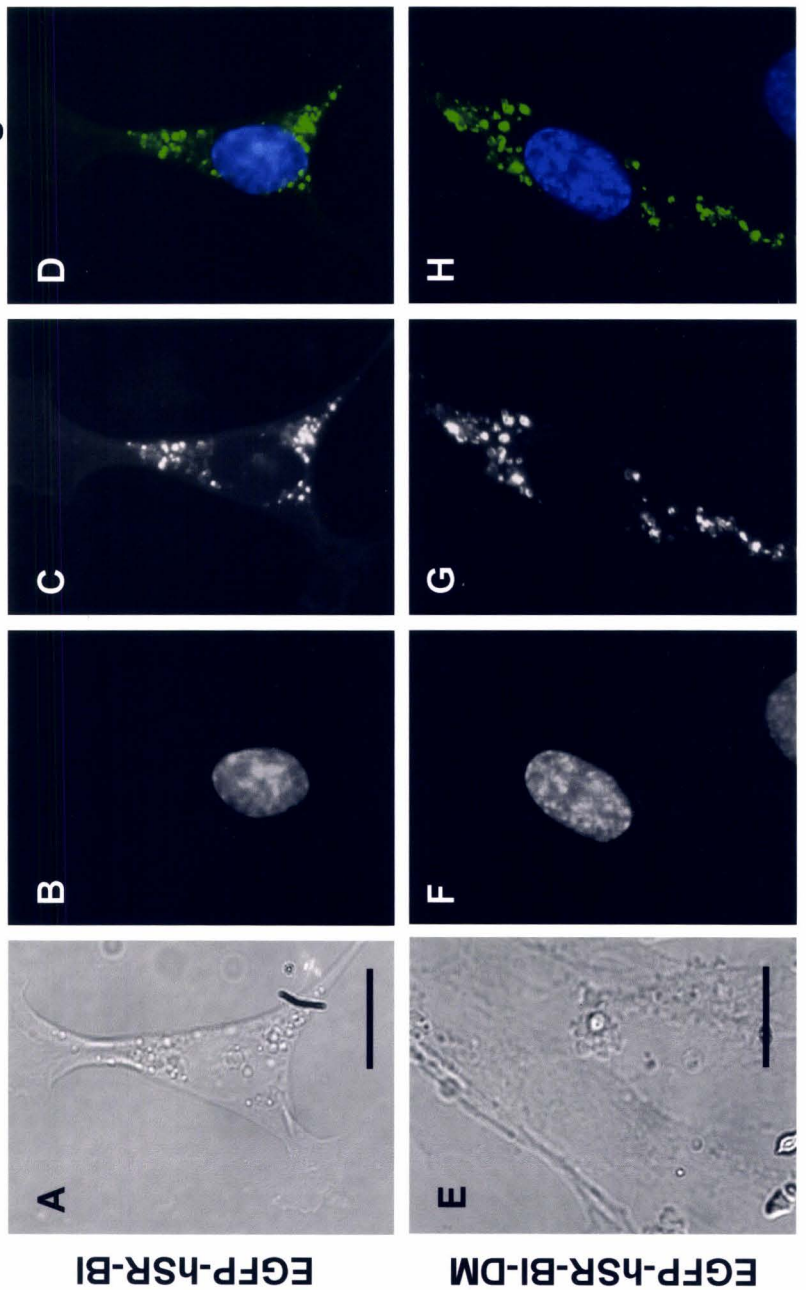


**Figure 2. Localization of EGFP-tagged hSR-BI containing or lacking the C-terminal tail in transfected HAEC.** HAEC transfected with EGFP-hSR-BI (A-D) or EGFP-hSR-BI-DM (E-H) were fixed after 24 hrs and stained with DAPI The cells were imaged by DIC microscopy (A & E) and by fluorescence microscopy in the blue (B & F, labeled DAPI) and green (C & G, labeled EGFP) channels. Merged images of the blue and green channels are shown in panels D and H. Scale bar = 10 μm. All images are at the same magnification. Representative images are shown. In HAEC both EGFP-hSR-BI and EGFP-hSR-BI-DM are localized to punctate structures within the cells.

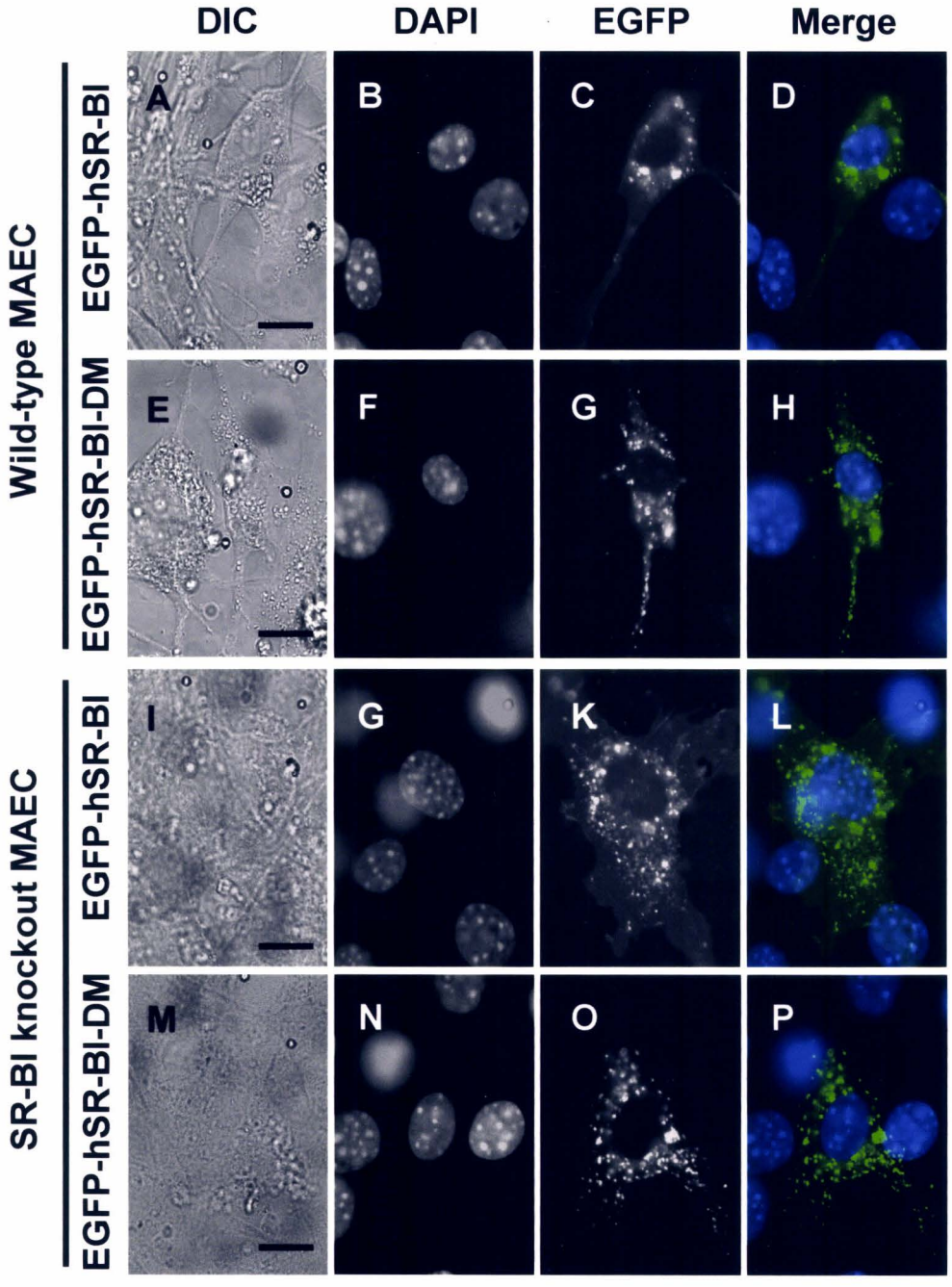
DIC
DAPI
EGFP
Merge
Wild-type MAEC
EGFP-hSR-BI
EGFP-hSR-BI-DM
SR-BI knockout MAEC
EGFP-hSR-BI
EGFP-hSR-BI-DM
A
B
C
D
E
F
G
H
I
G
K
L
M
N
O
P

**Figure 3. Localization of EGFP-tagged hSR-BI containing or lacking the C-terminal tail in transfected MAEC.** Wild-type (A-H) and SR-BI knockout (I-P) MAEC transfected with EGFP-hSR-BI (A-D & I-L) or EGFP-hSR-BI-DM (E-H & M-P) were fixed after 24 hrs and stained with DAPI. The cells were imaged by DIC microscopy (A, E, I & M) and by fluorescence microscopy in the blue (B, F, J & N, labeled DAPI) and green (C, G, K & O, labelled EGFP) channels. Merged images of the blue and green channels are shown in panels D, H, L and P. Scale bar = 10 μm. All images are at the same magnification. Representative images are shown. In wild-type and SR-BI knockout MAEC both EGFP-hSR-BI and EGFP-hSR-BI-DM are localized to punctate structures within the cells.

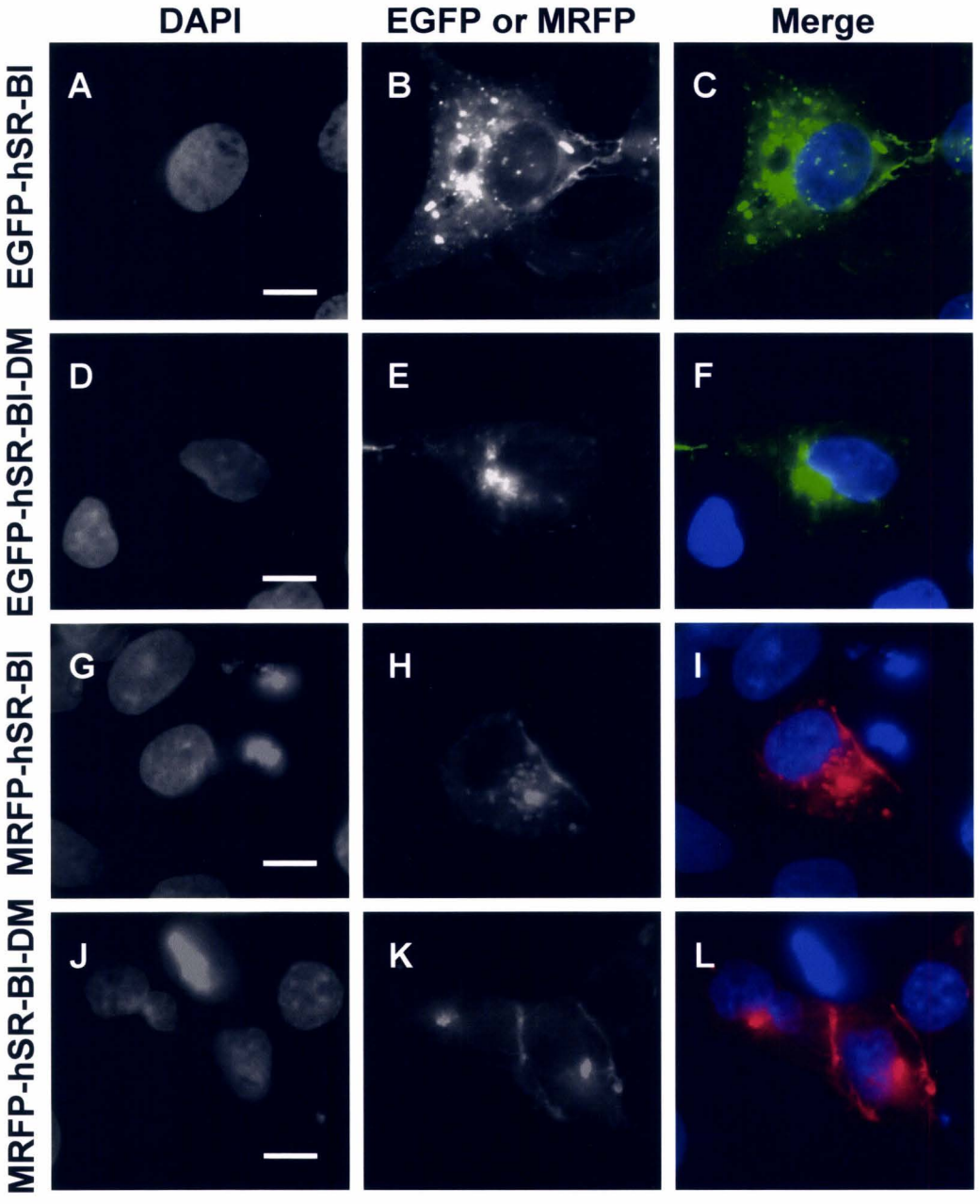
DAPI
EGFP or MRFP
Merge
EGFP-hSR-BI
EGFP-hSR-BI-DM
MRFP-hSR-BI
MRFP-hSR-BI-DM
A
B
C
D
E
F
G
H
I
J
K
L

**Figure 4. Localization of EGFP-tagged hSR-BI containing or lacking the C-terminal tail in transfected HepG2 cells.** HepG2 cells transfected with EGFP-tagged hSR-BI (A-C) or hSR-BI-DM (D-F) or MRFP-tagged hSR-BI (G-I) or hSR-BI-DM (J-L) were fixed after 48 hrs and stained with DAPI. The cells were imaged by fluorescence microscopy in the blue (A, D, G & J, labeled DAPI), green (B & E, labeled EGFP) and/or red (H & K, labeled MRFP) channels. Merged images of the blue and green (C & F) or the blue and red (I & L) channels are also shown. Scale bar = 10 μm. All images are at the same magnification. Representative images are shown. In HepG2 cells, EGFP or MRFP-tagged hSR-BI and hSR-BI-DM fusion proteins localize to the cell periphery, punctate structures and juxtanuclear regions.

fluorescently-tagged SR-BI was distributed in a reticular pattern reminiscent of the ER (data not shown). Fluorescence microscopy images of HepG2 cells co-transfected (refer to B.2. Methods) with EGFP-hSR-BI and MRFP-hSR-BI-DM or MRFP-hSR-BI and EGFP-hSR-BI-DM were also captured. Representative images of the transfected cells (Fig 5) show that the tagged full length and C-terminal truncation mutant hSR-BI proteins colocalize in HepG2 cells. Regions of colocalization appear in yellow. Hence, in HepG2 cells the distribution of SR-BI is not affected by the deletion of its C-terminal tail.

### C.1.2. Generation of HepG2 Cell Lines Stably Overexpressing EGFP-hSR-BI or EGFP-hSR-BI-DM

In order to determine the effects of SR-BI's C-terminal tail on the protein's function in hepatocytes, the lipid uptake activities of full length and C-terminal truncation mutant hSR-BI were determined. Since these experiments required cells overexpressing either hSR-BI or hSR-BI-DM, HepG2 cell lines stably expressing EGFP-tagged forms of the proteins were generated (refer to B.2. Methods). Lysates were prepared from the HepG2[EGFP-hSR-BI] and HepG2[EGFP-hSR-BI-DM] stable cell lines, as well as from untransfected and EGFP transfected HepG2, ldlA7 and ldlA[hSR-BI] cells (Fig 6, Lanes 1-6, respectively), subjected to SDS-PAGE and electrophoretically transferred to PVDF membrane (refer to B.2. Methods). An immunoblot for SR-BI (Fig 6A) showed bands corresponding to the size of EGFP-hSR-BI (~104 kDa) in the HepG2[EGFP-hSR-BI] lysate (Fig 6 lane 1) and to the size (~82 kDa) of untagged hSR-BI in the ldlA[hSR-BI] lysate (Fig 6 lane 6); however, no bands were visible in the HepG2[EGFP-hSR-BI-DM]

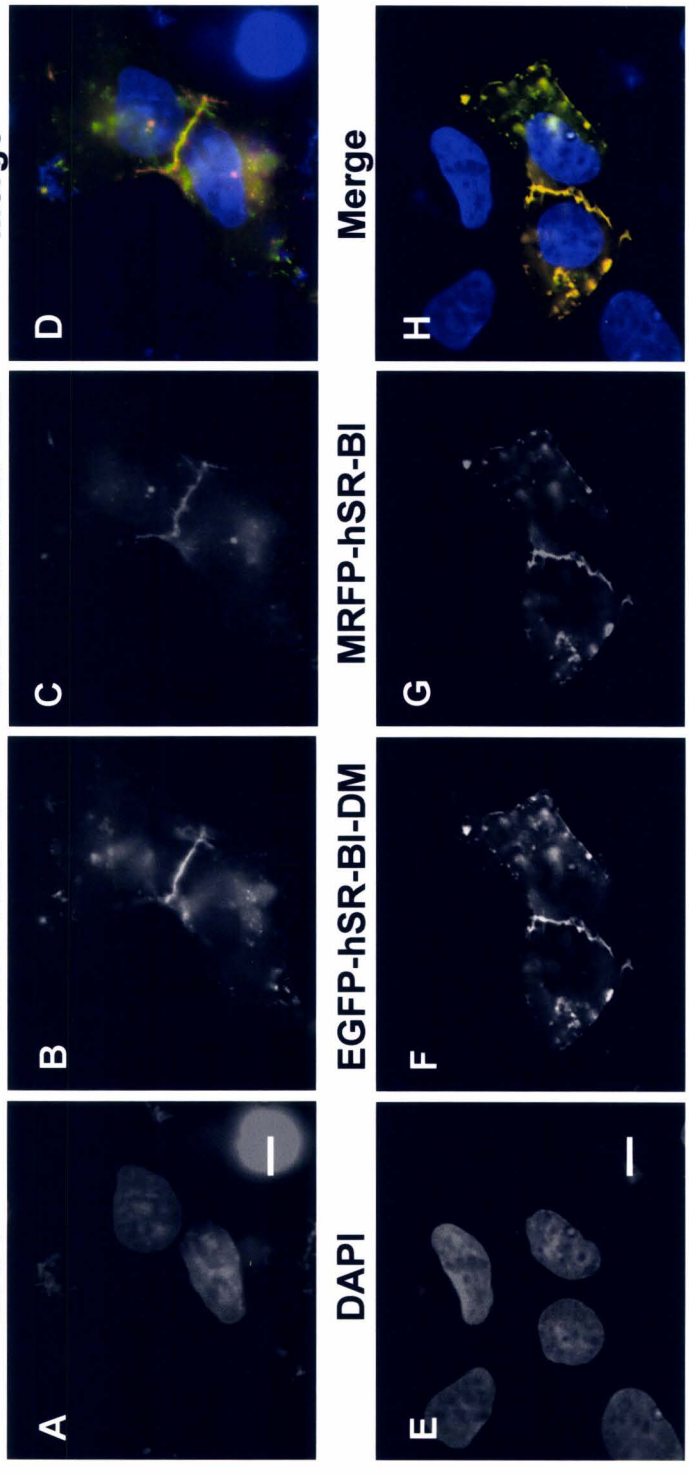


**Figure 5. Co-localization of EGFP-hSR-BI and mRFP-hSR-BI-DM or MRFP-hSR-BI and EGFP-hSR-BI-DM in HepG2 cells.** HepG2 cells cotransfected with EGFP-hSR-BI and MRFP-hSR-BI-DM (A-D) or MRPF-hSR-BI and EGFP-hSR-BI-DM (E-H) were fixed after 48 hrs and stained with DAPI. The cells were imaged by fluorescence microscopy in the blue (A & E), green (B & F) and red (C & G) channels. Merged images of the blue, green and red channels are shown in panels D & H. Scale bar = 10 μM. All images are at the same magnification. Representative images are shown. This data indicates that fluorescent protein tagged versions of hSR-BI and hSR-BI-DM colocalize in cells.

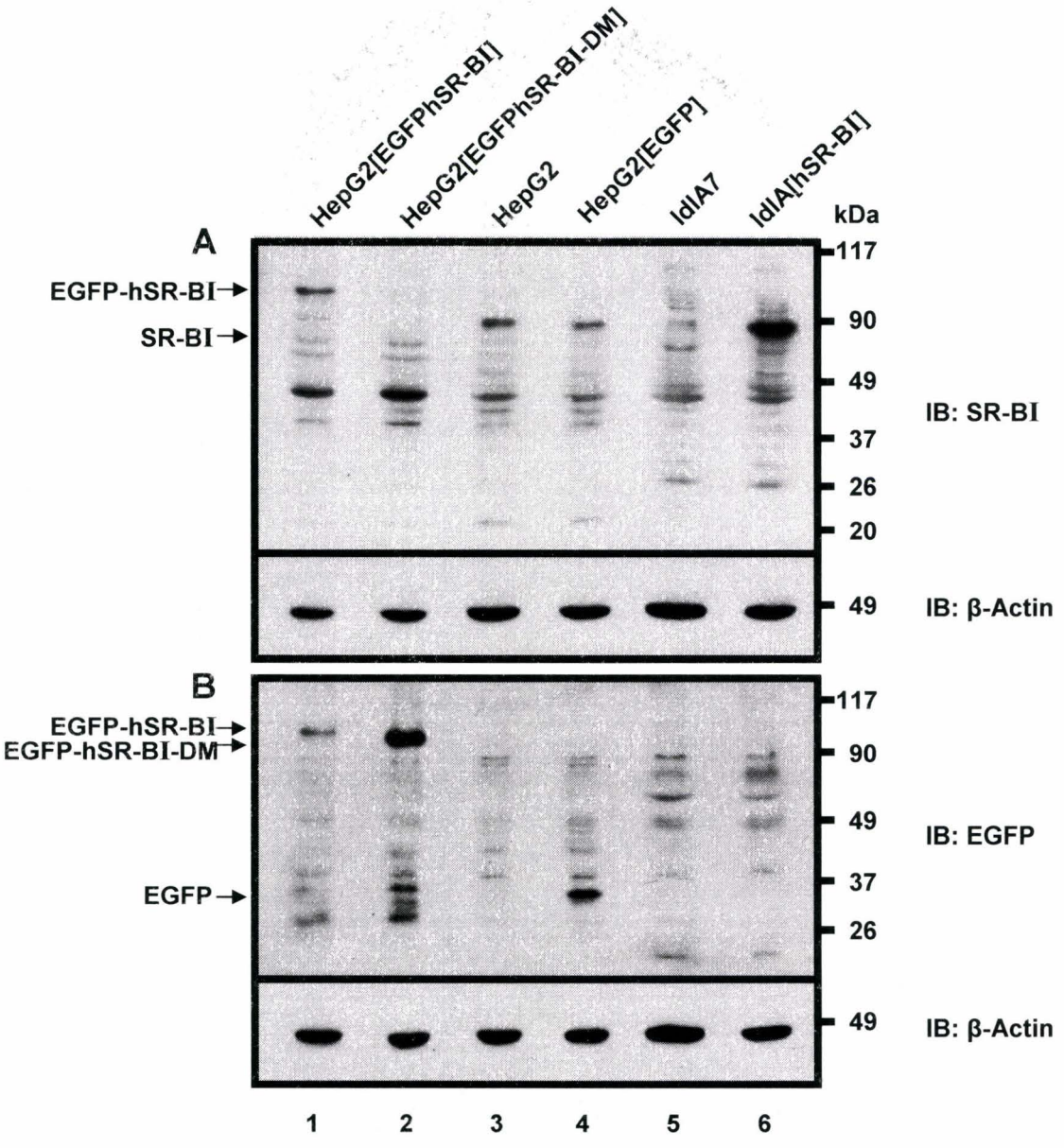


**Figure 6. Characterization of HepG2 cell lines stably expressing EGFP-tagged hSR-BI or EGFP-tagged hSR-BI-DM by immunoblotting for SR-BI and EGFP.** Cell lysates prepared from HepG2 cells stably expressing EGFP-hSR-BI (Lane 1) or EGFP-hSR-BI-DM (Lane 2), untranfected (Lane 3) and EGFP transfected (Lane 4) HepG2 cells, ldlA7 (Lane 5) and ldlA[hSR-BI] (Lane 6) were subjected to SDS-PAGE (8 and 12% separating gels). Immunoblotting for SR-BI (α C-terminal tail antibody) (A) and EGFP (B) was performed on the 8 and 12% gels, respectively. Immunoblotting for β-actin was also performed to serve as a loading control (A & B). Proteins of the expected sizes were detected, indicating that the fluorescence patterns observed in Figures 4 and 5 represented distribution patterns of fluorescent protein tagged hSR-BI.

lysate (Fig 6 lane 2) or in the ldlA7 lysate (Fig 6 lane 5). Hence, the protein expressed in the HepG2[EGFP-hSR-BI-DM] cells does not have a C-terminal tail since it was not recognized by the SR-BI antibody. The EGFP immunoblot (Fig 6B) showed bands of the size of EGFP-hSR-BI (~104 kDa) and EGFP-hSR-BI-DM (~96 kDa) in lysates from HepG2[EGFP-hSR-BI] (Fig 6 lane 1) and HepG2[EGFP-hSR-BI-DM] (Fig 6 lane 2) cells, respectively. A band corresponding to the size of EGFP was also seen in the lysate from HepG2 cells transfected with EGFP (Fig 6 lane 5). However, no distinct bands were seen in HepG2, ldlA7 or ldlA[hSR-BI] cell lysates (Fig 6 lanes 3 and 5, respectively). Therefore, the proteins expressed in the HepG2[EGFP-hSR-BI] and HepG2[EGFP-hSR-BI-DM] stable cell lines both have EGFP tags and are of the correct size.

### C.1.3. Role of SR-BI's C-terminal Tail in HDL-lipid Uptake

Once the stable cell lines were generated, the DiI-HDL lipid uptake activity in untransfected HepG2, HepG2[EGFP-hSR-BI] and HepG2[EGFP-hSR-BI-DM] cells was assayed (refer to B.2. Methods). DiI-HDL lipid specific uptake activities in the HepG2[EGFP-hSR-BI] and HepG2[EGFP-hSR-BI-DM] cells were 4 and 6 fold greater than that of untransfected control cells (Fig 7A). The EGFP fluorescence in the HepG2[EGFP-hSR-BI] cells was ~ 3 fold lower than that of the HepG2[EGFP-hSR-BI-DM] cells . Normalization of the DiI-HDL lipid specific uptake activities in each of the stable cell line to their EGFP fluorescences, giving normalization of activity to protein

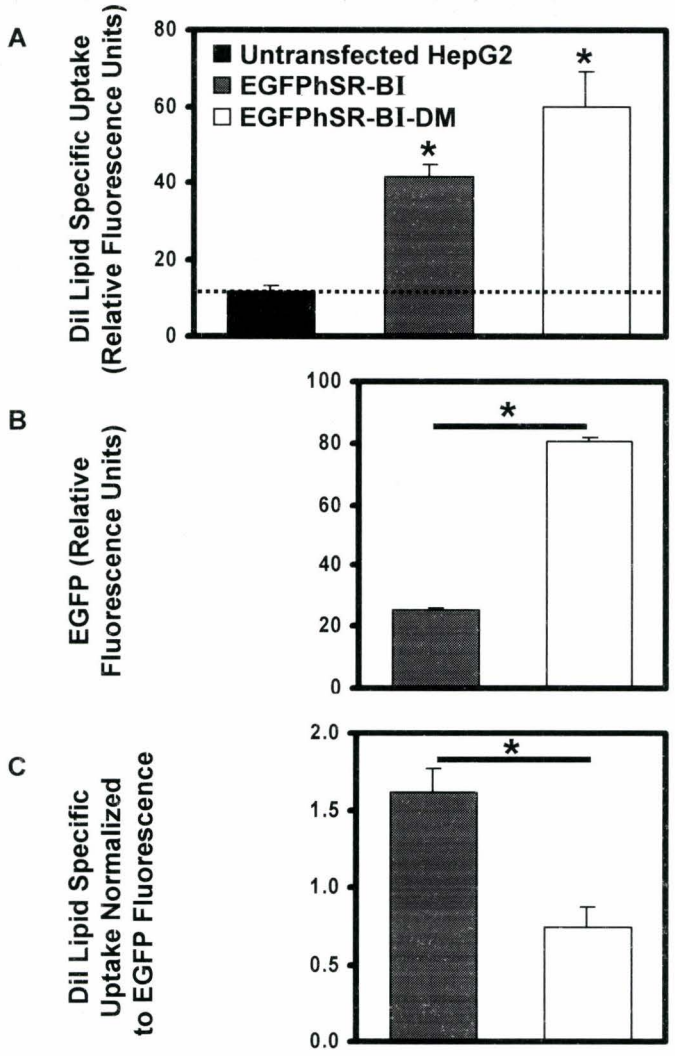


**Figure 7. Deletion of the C-terminal cytoplasmic tail of hSR-BI reduces but does not eliminate its lipid uptake activity.** A DiI-HDL lipid uptake assay was performed on HepG2, HepG2[EGFP-hSR-BI] and HepG2[EGFP-hSR-BI-DM] cells. The DiI and EGFP fluorescence of the samples was measured by flow cytometry. The specific uptake of DiI lipid in the 3 cell types are shown in panel A. The mean EGFP fluorescence and specific uptake of DiI lipid normalized to EGFP fluorescence of HepG2[EGFP-hSR-BI] and HepG2[EGFP-hSR-BI-DM] cells are shown in panels B and C, respectively. The experiment was performed in triplicate and error bars represent standard deviations. *$P<0.05$ (Student's *t*-test). Similar results were obtained when an independent clone of HepG2[EGFP-hSR-BI-DM] was analyzed (not shown). Although the steady state level of EGFP-hSR-BI-DM protein was greater than that of EGFP-hSR-BI (see also lanes 1 and 2 of Fig 6B) the level of HDL-lipid uptake was only slightly increased, suggesting that the deletion of the C-terminal cytoplasmic tail reduced but did not eliminate SR-BI HDL-lipid uptake activity.

expression, showed that the DiI-HDL lipid specific uptake activity in HepG2[EGFP-hSR-BI] cells was 2 fold greater than that in HepG2[EGFP-hSR-BI-DM] cells.

### C.1.4. Regulation of HDL-lipid Uptake Mediated by hSR-BI and hSR-BI-DM

Regulation of SR-BI's HDL-lipid uptake activity has been the focus of many studies. In particular, it was recently reported that murine or human SR-BI showed species specific sensitivities to inhibition of either PI3K or PKC in CHO cells (Zhang et al. b 2007). We therefore tested if hSR-BI's activity, in a physiologically relevant cell type such as hepatocytes, is regulated by PI3K or PKC signalling cascades. DiI-HDL lipid uptake assays (refer to B.2. Methods) were performed on HepG2[EGFP-hSR-BI] cells treated with wortmannin (PI3K inhibitor), PMA (PKC activator), calphostin C (PKC inhibitor), BLT-1 (SR-BI inhibitor) or combinations of these compounds. The effects of wortmannin on HDL-lipid uptake in HepG2[EGFP-hSR-BI] cells was tested repeatedly; however, no difference in activity was detected compared to untreated control cells (data not shown). Similarly, we saw no effects of either serum starvation or wortmannin on SR-BI's cell surface versus internal distribution, in contrast with a recent report from Shetty and collaborators (Shetty et al. 2006), but in agreement with data obtained in WIF-B cells by Harder and coworkers (Harder et al. 2007) (data not shown). On the other hand, treatment of the cells with PMA increased activity by ~30%, while calphostin C, a PKC inhibitor, decreased DiI-HDL lipid uptake in HepG2[EGFP-hSR-BI] cells by ~ 40% (Fig 8 A). For comparison, BLT-1, an SR-BI inhibitor identified in a high throughput screen for inhibitors of murine SR-BI-dependent HDL lipid uptake

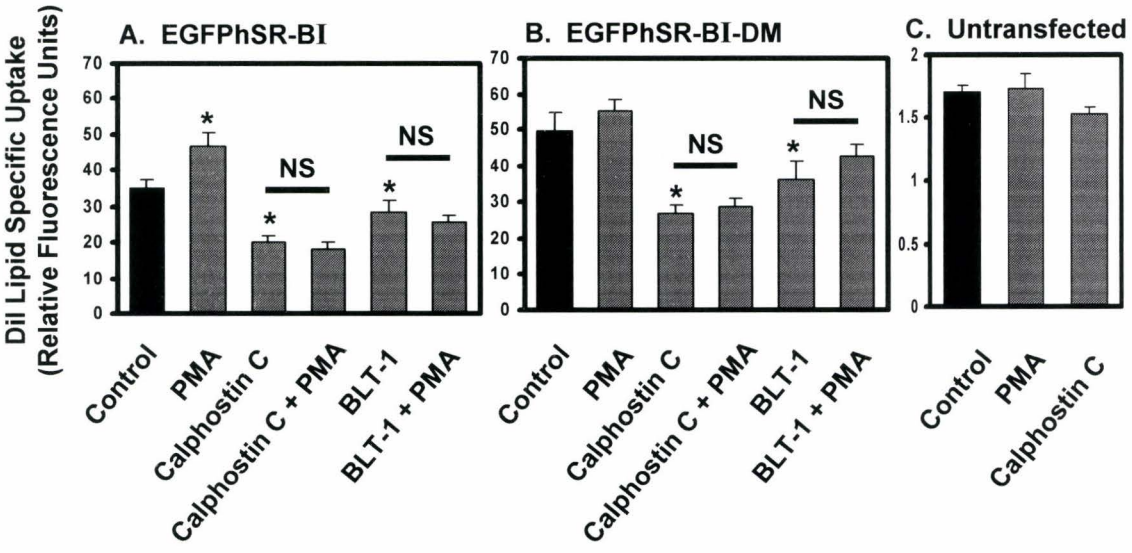


**Figure 8. The PKC inhibitor calphostin C reduces SR-BI-dependent HDL-lipid uptake independently of SR-BI's C-terminus.** DiI-HDL lipid uptake assays were performed on HepG2[EGFP-hSR-BI] (A), HepG2[hSR-BI-DM] (B) or untransfected HepG2 cells (C) treated with 0.5 μM PMA, 1 μM calphostin C, 300 nM BLT-1 as indicated for 10 min prior to and during the 2 hr incubation with DiI-HDL. The cellular DiI fluorescence was measured by flow cytometry. The activity was expressed as specific uptake of DiI lipid. Experiments were performed in triplicate and error bars represent standard deviations. *$P<0.05$ for control cells compared to treated cells. PMA or calphostin C treatment did not affect background HDL-lipid uptake in untransfected HepG2 cells (C), note the expanded scale of the y axis compared to panels A and B. Calphostin C treatment significantly reduced HDL-lipid uptake mediated by hSR-BI (A) as well as hSR-BI-DM (B). PMA treatment only slightly increased HDL-lipid uptake by hSR-BI. These data suggest that PKC inhibition reduces hSR-BI mediated HDL-lipid uptake in HepG2 cells, independently of the C-terminal cytoplasmic region.

in CHO cells, reduced DiI-HDL lipid uptake by ~20%. The effect of PMA was inhibited when the cells were also treated with calphostin C or BLT-1 (Fig 8 A). To determine if the C-terminal tail of SR-BI was required for the effects on SR-BI HDL-lipid uptake, the experiment was repeated using HepG2[EGFP-hSR-BI-DM] cells. Calphostin C and BLT-1 each inhibited DiI-HDL lipid specific activity by ~ 50 and 25%, respectively (Fig 8 B); however, no significant increase in activity was detected when the cells were treated with PMA (Fig 8 B). DiI-HDL lipid uptake by untransfected HepG2 cells (Fig 8C) was substantially lower (only 5%) of that by HepG2[EGFP-hSR-BI] or HepG2[EGFP-hSR-BI-DM] cells and was not affected by either PMA or calphostin C treatment. This confirmed that the PMA-mediated increase and calphostin C or BLT-1-dependent decreases in DiI-HDL lipid uptake reflected SR-BI-dependent activity.

## C.2. Generation of Transgenic Mice with Liver-specific Expression of hSR-BI or hSR-BI-DM

### C.2.1. Generation of $pP_{TRE}$hSR-BI and $pP_{TRE}$hSR-BI-DM Constructs

Studies focused on the overexpression or attenuation/elimination of mSR-BI in mice have demonstrated SR-BI's atheroprotective role (Kozarsky et al. 1997; Rigotti et al. 1997; Varban et al. 1998; Wang et al. 1998; Ueda et al. 1999; Huby et al. 2006), as well as its importance in the clearance of HDL cholesterol by the liver (Arai et al. 1999; Trigatti et al. 1999; Huszar et al. 2000; Kozarsky et al. 2000; Ueda et al. 2000; Covey et al. 2003). A recent study conducted in ldlA7 cells stably overexpressing mSR-BI or hSR-BI has shown that the regulation of the activity and the mechanisms of lipid

internalization of murine and human SR-BI proteins differ (Zhang et al. b 2007). Hence, the effects of hSR-BI overexpression in mice may vary from those observed in mice overexpressing the murine ortholog of the protein. Research has also shown that the C-terminal cytoplasmic region of SR-BI (Yuhanna et al. 2001) or expression of PDZK1 (Kimura et al. 2006), which binds to SR-BI's C-terminus (Silver 2002), are required in order for the protein to activate various signalling pathways and downstream processes which may have atheroprotective effects. In view of this data, we wanted to determine the effects of human SR-BI and its C-terminal tail on the development of atherosclerosis, and on lipoprotein metabolism in mice.

Since assessing the effects of SR-BI overexpression in various tissues was of interest, we decided to use a bipartite tetracycline expression system, which requires driver and responder transgenes, to generate mice with tissue-specific and regulatable overexpression of either full length or deletion mutant hSR-BI. The driver transgene consists of a tissue-specific promoter upstream of a tetracycline transactivator (tTA), while the responder transgene consists of a bidirectional promoter made up of 2 minimal cytomegalovirus (CMV) promoters and a tetracycline responsive element (TRE) between oppositely oriented cDNA's encoding the protein of interest and β-galactosdase as a marker for expression. Expression of the proteins is inhibited in the presence of tetracycline or its derivative, doxycycline (Martin et al. 1969; Gossen et al. 1992).

To determine the effects of hSR-BI overexpression in the liver, as well as to extend our *in vitro* studies into the role of the C-terminal cytoplasmic tail of hepatic SR-BI into a mouse model, we chose to use a liver-specific driver line. The mouse line, consisting of the major urinary protein promoter upstream of the tTA ($P_{MUP}$tTA) (Kawamura et al. 1997), was obtained from Dr T. Jake Liang at the National Institutes of Health. To generate mice expressing the responder transgenes, hSR-BI and hSR-BI-DM were first cloned into the pBIGN2 vector (obtained from Dr. Mansour Husain from the University of Toronto) (refer to B.2. Methods) to give $pP_{TRE}$hSR-BI and $pP_{TRE}$hSR-BI-DM, respectively (Fig 9) and the functionality of the constructs were tested *in vitro*.

### C.2.2. Characterization of $pP_{TRE}$hSR-BI and $pP_{TRE}$hSR-BI-DM Constructs *In Vivo*

To verify that the responder transgenes led to expression of hSR-BI or hSR-BI-DM and that the system could be regulated by doxycycline, a tetracycline derivative, cells were transfected with pTet-Off (CMV promoter upstream of tTA) and $pP_{TRE}$hSR-BI or $pP_{TRE}$hSR-BI-DM, respectively (refer to B.2. Methods) and grown in the presence or absence of 10 μg/mL doxycycline. Lysates were prepared from the cells and subjected to SDS-PAGE. Immunoblotting for SR-BI was performed. Cells transfected with pTet-Off and $pP_{TRE}$hSR-BI or $pP_{TRE}$hSR-BI-DM expressed hSR-BI or hSR-BI-DM, respectively, when cultured in the absence, but not in the presence of doxycycline (shown in Fig 10A & B, respectively). To verify that the lacZ reporter gene encoded a functional β-galactosidase enzyme and that its expression could be regulated by doxycycline, cells were transfected with pTet-Off and $pP_{TRE}$hSR-BI, $pP_{TRE}$hSR-BI-DM or pBIGN2 (refer to

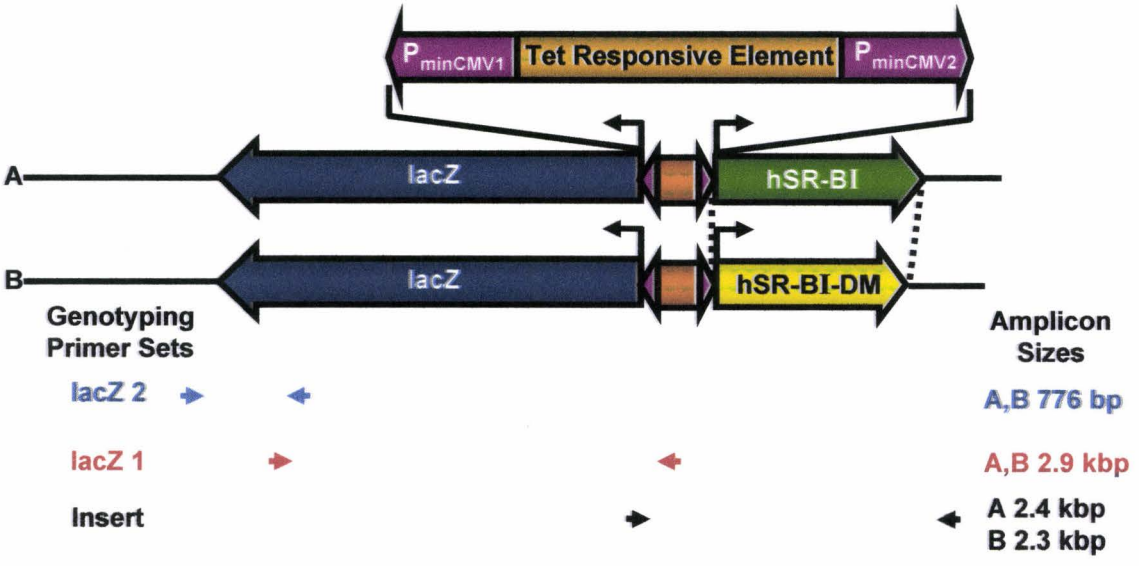


**Figure 9. Structures of the $P_{TRE}$hSR-BI and $P_{TRE}$hSR-BI-DM transgenes.** The $P_{TRE}$hSR-BI and $P_{TRE}$hSR-BI-DM transgenes both consist of a bidirectional promoter, comprised of a tetracycline responsive element (TRE) flanked by two minimal cytomegalovirus (CMV) promoters, located upstream of hSR-BI or hSR-BI-DM and lacZ transgenes. The locations of three primer sets (Insert, lacZ 1 and lacZ 2) designed to span the entire region of interest, as well as their amplicon sizes, are indicated. These primers were used to characterize the inserts in different lines of transgenic mice obtained (see Fig 11).

A

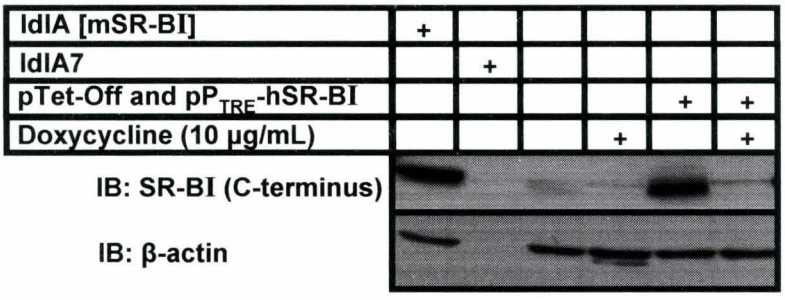


B

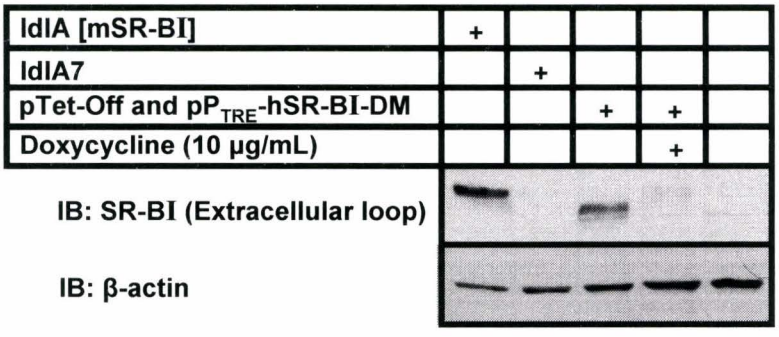


C

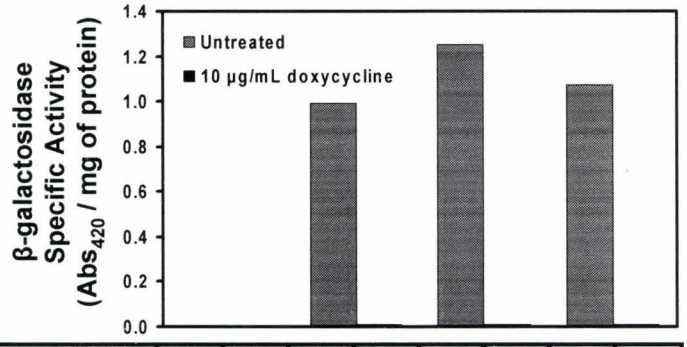


| Doxycycline (10 µg/mL) | - | + | - | + | - | + | - | + |
|---|---|---|---|---|---|---|---|---|
| pTet-Off | - | - | + | + | + | + | + | + |
| pP$_{TRE}$-hSR-BI | - | - | + | + | - | - | - | - |
| pP$_{TRE}$-hSR-BI-DM | - | - | - | - | + | + | - | - |
| pBIGN2 | - | - | - | - | - | - | + | + |

**Figure 10. Test of tet-off driven expression of β-galactosidase and either hSR-BI or hSR-BI lacking the C-terminal tail in transfected cells in culture.** 3T3-L1 (A) and HEK 293 (B & C) cells were transfected with pTet-Off and pPTREhSR-BI, pPTREhSR-BI-DM or pBIGN2 (empty vector) and cultured for 48 hrs, the last 40 hrs of which was in the presence or absence of 10 μg / mL doxycycline as indicated. LdlA[mSR-BI] cells which overexpress mSR-BI, and untransfected ldlA7 cells which express undetectable levels of SR-BI were used as positive and negative controls for SR-BI expression. Lysates were prepared and subjected to SDS-PAGE and immunoblotting for SR-. Antibodies raised against the C-terminus (A) or the extracellular loop (B) were used for cells transfected with pPTREhSR-BI (A) or pPTREhSR-BI-DM (B), respectively. Immunoblotting for β-actin was also performed to serve as a loading control. Cell lysates were assayed for β-galactosidase activity using ONPG as the substrate (C). The pPTREhSR-BI and pPTREhSR-BI-DM constructs lead to expression of hSR-BI or hSR-BI-DM protein, respectively, and of functional β-galactosidase.

B.2. Methods) and cultured in the presence or absence of 10 μg/mL doxycycline. Cell lysates were prepared and assayed for β-galactosidase activity. The cells transfected with pTet-Off and $pP_{TRE}$hSR-BI, $pP_{TRE}$hSR-BI-DM or pBIGN2 and then cultured in the absence of the antibiotic showed β-galactosidase specific activities of 1.0, 1.3 and 1.1 $Abs_{420}$/mg of protein, respectively (Fig 10C). However, cells cultured in the presence of doxycycline did not express detectable β-galactosidase activity (Fig 10C).

### C.2.3. Generation of $P_{TRE}$hSR-BI and $P_{TRE}$hSR-BI-DM Responder Mice

The $pP_{TRE}$hSR-BI and $pP_{TRE}$hSR-BI-DM vectors were digested with Not I and prepared for the generation of transgenic mice (refer to B.2. Methods). Pronuclear injections of the $P_{TRE}$hSR-BI and $P_{TRE}$hSR-BI-DM transgenes were conducted by the London Transgenic and Gene Targeting Facility and by Aline Fiebig, a technician in Dr Suleiman Igdoura's laboratory at McMaster University, respectively. Through these procedures, 37 potential founders were obtained for both the $P_{TRE}$hSR-BI and $P_{TRE}$hSR-BI-DM mouse lines. Initial genotyping of the mice, performed by Heather Gray, showed 2 potential founders for both the $P_{TRE}$hSR-BI (lines 262 and 268) and $P_{TRE}$hSR-BI-DM (lines 608 and 4766) transgenic mouse lines (data not shown).

To verify that the entire transgene of interest was incorporated into the genome of each of these mice, further PCR genotyping (refer to B.2. Methods) was conducted using 1 primer set (insert) which amplified either hSR-BI or hSR-BI-DM in $P_{TRE}$hSR-BI and $P_{TRE}$hSR-BI-DM, respectively, and 2 primer sets (lacZ 1 and lacZ 2) which together

amplified the lacZ gene in its entirety. The location of the annealing sites of the primers and the amplicon sizes are indicated in Fig 9. The expected PCR products based on the predicted fragment sizes (Fig 9) were obtained for all 4 potential transgenic founders. DNA from the founders of lines 262 and 268 ($P_{TRE}$hSR-BI) and lines 608 and 4766 $P_{TRE}$hSR-BI-DM gave products of ~ 2.4 and 2.3 kbp, respectively, in the reactions performed using the insert primer set (Fig 11). While DNA from all founders gave PCR products of ~ 2.9 kbp and 800 bp for reactions conducted using the lacZ 1 and lacZ 2 primer sets, respectively (Fig 11). Non-specific bands seen in the reactions conducted with the lacZ 1 primer set and DNA from the founders of lines 608 and 4766 were not of the expected size and were also seen in the reaction conducted with a negative control (wild-type mouse genomic DNA). Hence, the $P_{TRE}$hSR-BI (lines 262 and 268) and $P_{TRE}$hSR-BI-DM (lines 608 and 4766) transgenic mouse lines have the correct inserts.

### C.2.4. Characterization of $P_{MUP}$tTA / $P_{TRE}$hSR-BI and $P_{MUP}$tTA / $P_{TRE}$hSR-BI-DM Transgenic Mice

#### C.2.4.1. Determination of Hepatic Promoter Activity

Since the potential founders of the $P_{TRE}$hSR-BI (262 and 268) and $P_{TRE}$hSR-BI-DM (608 and 4766) mouse lines expressed the desired transgenes in their entireties, each was mated to the $P_{MUP}$tTA driver mouse lines in order to generate $P_{MUP}$tTA / $P_{TRE}$hSR-BI and $P_{MUP}$tTA / $P_{TRE}$hSR-BI-DM double transgenic mice and single transgenic littermate controls. The mouse husbandry and genotyping were conducted by Heather Gray. At ten weeks of age, the mice were harvested (refer to B.2. Methods). In order to determine if

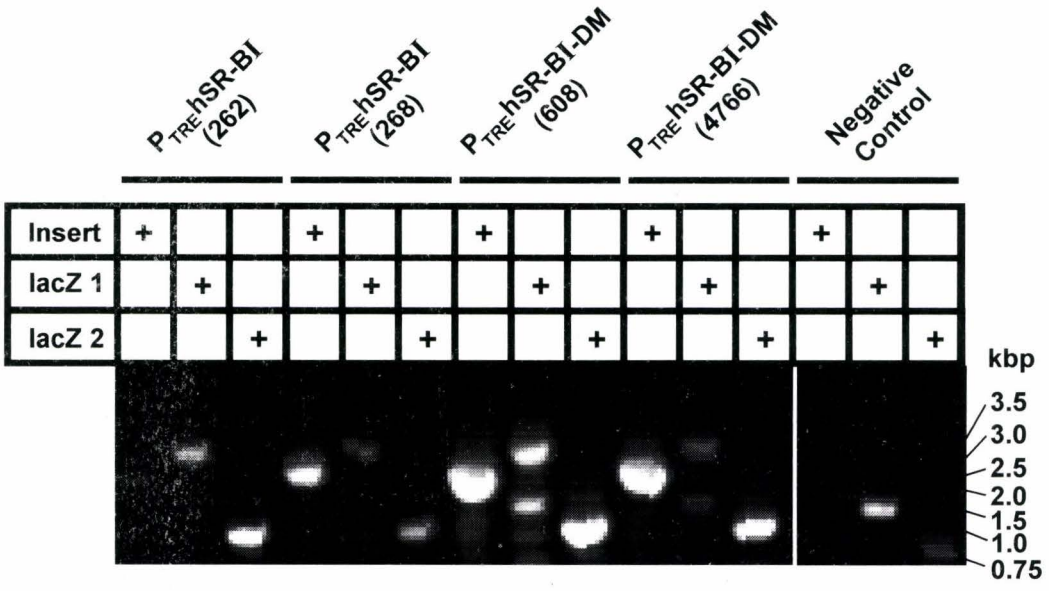


**Figure 11. PCR characterization of inserts in different lines of transgenic mice.** Potential founders of the $P_{TRE}$hSR-BI and $P_{TRE}$hSR-BI-DM mouse lines were tested to verify the presence of the entire transgenes of interest. PCR was conducted using tail genomic DNA, a primer set to detect hSR-BI or hSR-BI-DM (insert) and 2 primer sets which together detect the entire lacZ sequence (lacZ 1 and lacZ 2). The locations of these primer sets are displayed in Figure 9. $P_{TRE}$hSR-BI (lines 262 and 268) and $P_{TRE}$hSR-BI-DM (lines 608 and 4766) mice contain the transgenes of interest in their entireties.

the promoters were active and to verify that activity detected was dependent on the presence of both the driver and responder transgenes, the β-galactosidase activity in the liver of the $P_{MUP}$tTA / $P_{TRE}$hSR-BI and $P_{MUP}$tTA / $P_{TRE}$hSR-BI-DM double transgenic mice and single transgenic littermate controls was determined. The livers of the mice were homogenized and β-galactosidase activity was measured (rfer to B.2. Methods). β-galactosidase activity was detected in the livers of $P_{MUP}$tTA / $P_{TRE}$hSR-BI (line 268) (Fig 12A) and $P_{MUP}$tTA / $P_{TRE}$hSR-BI-DM (line 4766) (Fig 12B) double transgenic mice. No significant enzyme activity was detected in the livers of $P_{MUP}$tTA, $P_{TRE}$hSR-BI (lines 262 and 268) and $P_{TRE}$hSR-BI-DM (lines 608 and 4766) single transgenic mice, nor in the livers of $P_{MUP}$tTA / $P_{TRE}$hSR-BI (line 262) and $P_{MUP}$tTA / $P_{TRE}$hSR-BI-DM (line 608) double transgenic mice (Fig 12A & B).

### C.2.4.2. Assessment of Tissue Specificity of Promoter Activity

In order to verify that the activity of the promoters were restricted to the livers of the $P_{MUP}$tTA / $P_{TRE}$hSR-BI (line 268) and $P_{MUP}$tTA / $P_{TRE}$hSR-BI-DM (line 4766) double transgenic mice, lysates were prepared from a variety of tissues (adipose tissue, adrenal gland, brain, heart, intestine, kidney, lung, skeletal muscle, spleen and stomach) from $P_{MUP}$tTA / $P_{TRE}$hSR-BI (line 268) or $P_{MUP}$tTA / $P_{TRE}$hSR-BI-DM (line 4766) double transgenic mice and single transgenic controls and β-galactosidase activities were assayed. With the exception of the livers from the double transgenic mice no significant enzyme activity was detected in the tissue lysates prepared from $P_{MUP}$tTA / $P_{TRE}$hSR-BI (line 268) double transgenic mice and single transgenic controls (Fig 13A). The tissue

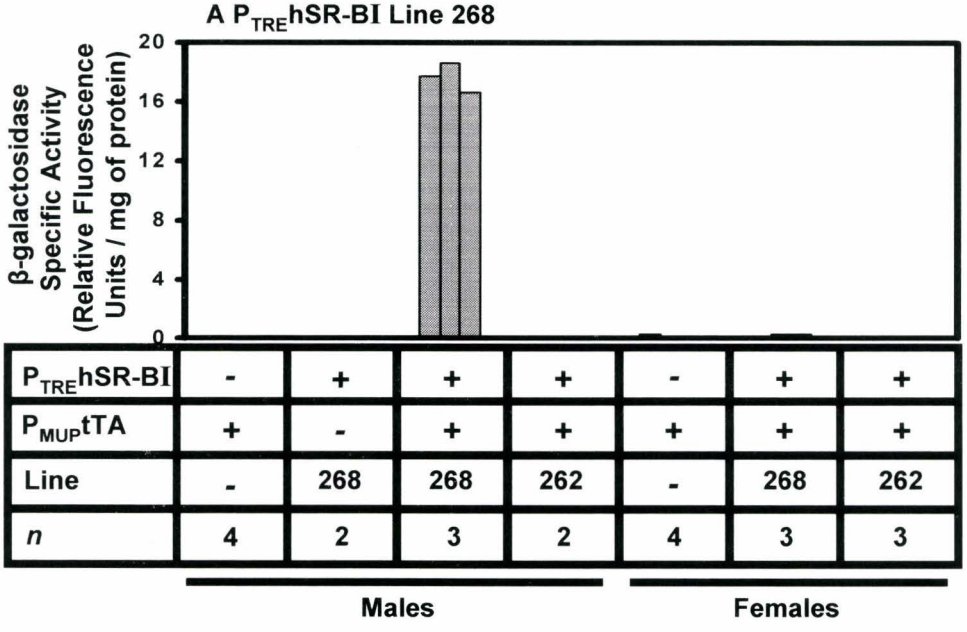


| | | | | | | | |
|---|---|---|---|---|---|---|---|
| P$_{TRE}$hSR-BI | - | + | + | + | - | + | + |
| P$_{MUP}$tTA | + | - | + | + | + | + | + |
| Line | - | 268 | 268 | 262 | - | 268 | 262 |
| *n* | 4 | 2 | 3 | 2 | 4 | 3 | 3 |

Males Females

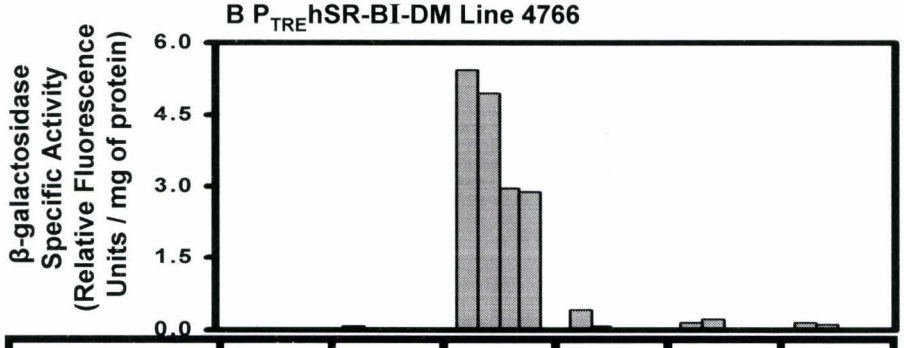


| | | | | | | |
|---|---|---|---|---|---|---|
| P$_{TRE}$hSR-BI-DM | - | + | + | + | + | + |
| P$_{MUP}$tTA | + | - | + | + | - | + |
| Line | - | 4766 | 4766 | 608 | 608 | 608 |
| *n* | 3 | 2 | 4 | 2 | 2 | 2 |

Males Females

**Figure 12. β-galactosidase activities in liver extracts from $P_{MUP}$tTA / $P_{TRE}$hSR-BI and $P_{MUP}$tTA / $P_{TRE}$hSR-BI-DM double transgenic mice and control mice.** Liver homogenates were prepared from 10 week old $P_{MUP}$tTA / $P_{TRE}$hSR-BI (A) and $P_{MUP}$tTA / $P_{TRE}$hSR-BI-DM (B) double transgenic mice, as well as from $P_{MUP}$tTA (A & B) and $P_{TRE}$hSR-BI (A) or $P_{TRE}$hSR-BI-DM (B) single transgenic control mice. β-galactosidase activity was assayed using CUG as the substrate. $P_{MUP}$tTA / $P_{TRE}$hSR-BI (line 268) and $P_{MUP}$tTA / $P_{TRE}$hSR-BI-DM (line 4766) double transgenic mice express β-galactosidase in their livers. Only one of each of the two double transgenic lines expressed β-galactosidase activities in their livers. Note the higher level of activity in the livers of double transgenic lines 268 ($P_{MUP}$tTA / $P_{TRE}$hSR-BI) than line 4766 ($P_{MUP}$tTA / $P_{TRE}$hSR-BI-DM).

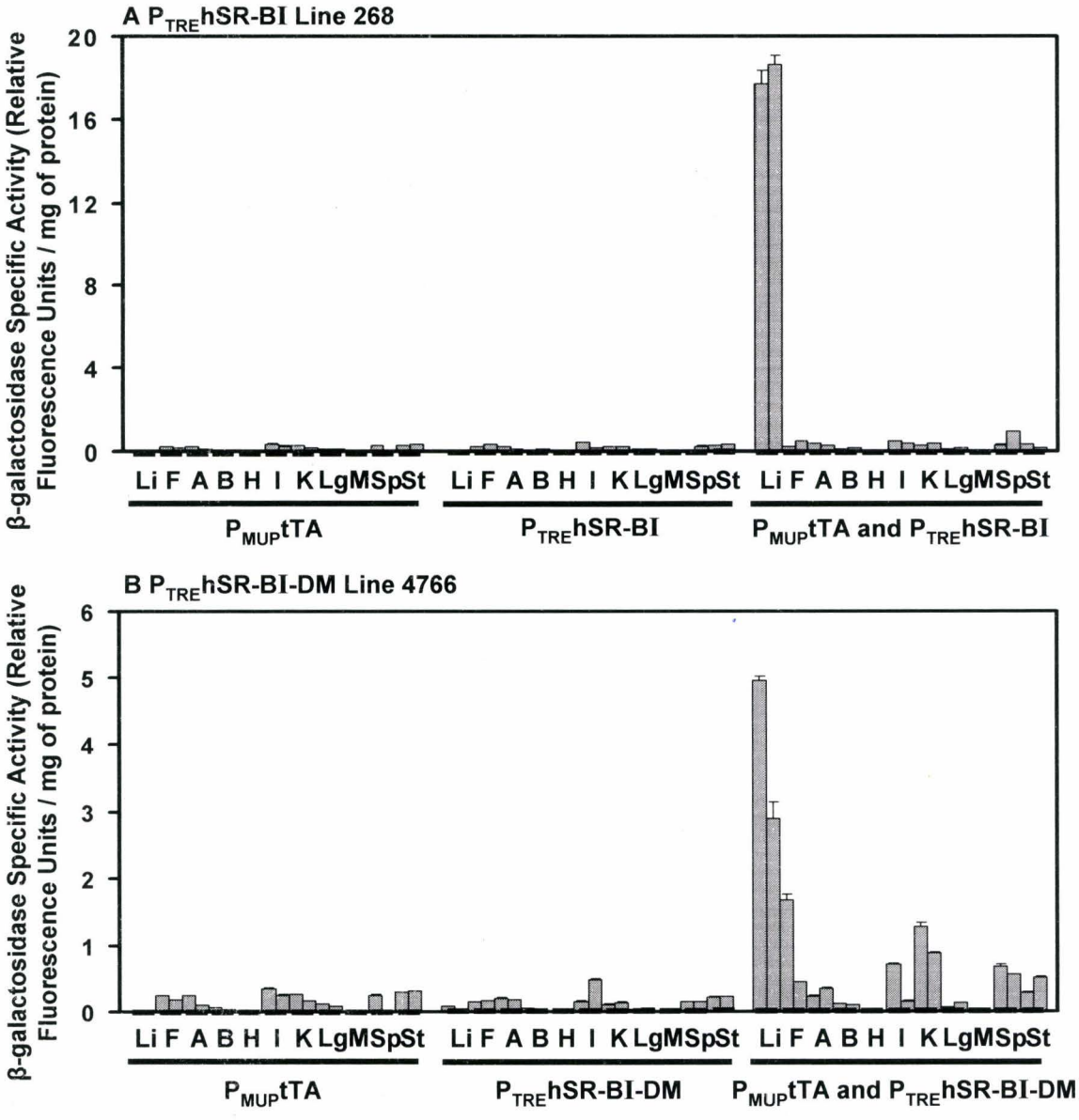


**Figure 13. β-galactosidase activities in different tissues of $P_{MUP}$tTA / $P_{TRE}$hSR-BI and $P_{MUP}$tTA / $P_{TRE}$hSR-BI-DM double transgenic mice and control mice.** Liver (Li), adipose tissue (F), adrenal gland (A), brain (B), heart (H), intestine (I), kidney (K), lung (L), skeletal muscle (M), spleen (Sp) and stomach (St) homogenates prepared from 10 week old $P_{MUP}$tTA / $P_{TRE}$hSR-BI (A) and $P_{MUP}$tTA / $P_{TRE}$hSR-BI-DM (B) double transgenic mice, as well as from $P_{MUP}$tTA (A & B) and $P_{TRE}$hSR-BI (A) or $P_{TRE}$hSR-BI-DM (B) single transgenic control mice. β-galactosidase activity was assayed using CUG as the substrate. $P_{MUP}$tTA / $P_{TRE}$hSR-BI (line 268) and $P_{MUP}$tTA / $P_{TRE}$hSR-BI-DM (line 4766) double transgenic mice express β-galactosidase specifically within their livers.

homogenates from the $P_{MUP}$tTA and $P_{TRE}$hSR-BI-DM (line 4766) did not have significant β-galactosidase activity (Fig 13B); however, the adipose tissue, intestines, kidneys, spleens and stomachs of $P_{MUP}$tTA / $P_{TRE}$hSR-BI-DM (line 4766) double transgenic mice had low levels of enzyme activity (Fig 13B) in comparison to liver lysates from mice of the same genotype.

### C.2.4.3. Determination of Total and HDL Cholesterol Levels in Plasma

Given that the promoters in the $P_{MUP}$tTA / $P_{TRE}$hSR-BI (line 268) or $P_{MUP}$tTA / $P_{TRE}$hSR-BI-DM (line 4766) double transgenic mice were active, the possible effects of overexpression of hSR-BI or hSR-BI-DM, respectively, in the mice were assessed. Hepatic overexpression of mSR-BI in mice causes a decrease in total cholesterol levels, as well as the elimination of cholesterol in HDL-sized particles (Kozarsky et al. 1997; Wang et al. 1998; Ueda et al. 1999; Huby et al. 2006). To determine if a similar effect was occurring in $P_{MUP}$tTA / $P_{TRE}$hSR-BI (line 268) or $P_{MUP}$tTA / $P_{TRE}$hSR-BI-DM (line 4766) double transgenic mice, plasma samples (prepared as described in B.2. Methods) from these mice as well as from single transgenic controls were assayed for total cholesterol (refer to B.2. Methods). The data obtained is preliminary due to the small sample size from each genotype and background tested. Based on the data obtained to date, no obvious differences in total cholesterol levels due to the presence of both $P_{MUP}$tTA and $P_{TRE}$hSR-BI (line 268) or $P_{TRE}$hSR-BI-DM (line 4766) were observed (Fig 14). The lipoprotein profiles generated from the plasma samples (refer to B.2. Methods) of these same mice yielded similar results. No obvious differences in HDL cholesterol

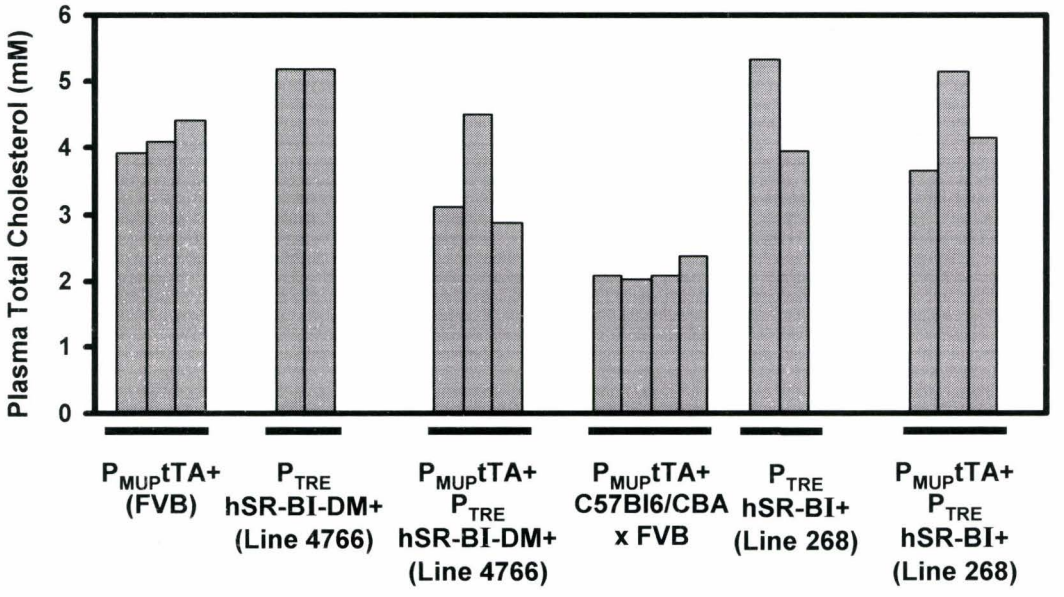


**Figure 14. Plasma total cholesterol levels of $P_{MUP}$tTA / $P_{TRE}$hSR-BI and $P_{MUP}$tTA / $P_{TRE}$hSR-BI-DM double transgenic mice and control mice.** Plasma samples from overnight fasted 10 week old $P_{MUP}$tTA / $P_{TRE}$hSR-BI and $P_{MUP}$tTA / $P_{TRE}$hSR-BI-DM double transgenic mice, as well as from $P_{MUP}$tTA and $P_{TRE}$hSR-BI or $P_{TRE}$hSR-BI-DM, single transgenic control mice, were assayed for total cholesterol levels. Plasma total cholesterol levels were not decreased in $P_{MUP}$tTA / $P_{TRE}$hSR-BI (line 268) or $P_{MUP}$tTA / $P_{TRE}$hSR-BI-DM (4766) double transgenic mice.

were observed for $P_{MUP}$tTA / $P_{TRE}$hSR-BI (line 268) (Fig 15) and $P_{MUP}$tTA / $P_{TRE}$hSR-BI-DM (line 4766) (Fig 16) double transgenic mice, except one mouse of the latter genotype (Fig 16, filled circles) which showed no HDL cholesterol peak and a small VLDL peak.

### C.2.4.4. Detection of hSR-BI and hSR-BI-DM mRNA Transcripts

Seeing as no phenotype was observed in the $P_{MUP}$tTA / $P_{TRE}$hSR-BI (line 268) (Fig 15) and $P_{MUP}$tTA / $P_{TRE}$hSR-BI-DM (line 4766) (Fig 16) mice, the presence of mRNA transcripts for hSR-BI and hSR-BI-DM, respectively, was verified. RNA was prepared from livers of $P_{MUP}$tTA / $P_{TRE}$hSR-BI (line 268) and $P_{MUP}$tTA / $P_{TRE}$hSR-BI-DM (line 4766) double transgenic mice and single transgenic controls and used to synthesize cDNA (refer to B.2. Methods). PCR was conducted using primers to amplify a portion of full length or C-terminal truncation mutant hSR-BI and murine β-actin (refer to B.2. Methods). Products of ~80 bp, were detected in the reactions conducted using the hSR-BI and DNA synthesized from the RNA of $P_{MUP}$tTA / $P_{TRE}$hSR-BI (line 268) mice only (Fig 17). However, murine β-actin was dectected in all of the samples, except the negative control to which no cDNA was added, indicating that cDNA was present in all of the experimental samples.

### C.2.4.5. Analysis of hSR-BI and hSR-BI-DM Protein Expression

Since mRNA transcripts of hSR-BI were detected in livers of $P_{MUP}$tTA / $P_{TRE}$hSR-BI (line 268) mice and β-galactosidase activity was detected in the livers of $P_{MUP}$tTA / $P_{TRE}$hSR-BI (line 268) and $P_{MUP}$tTA / $P_{TRE}$hSR-BI-DM (line 4766) mice, the

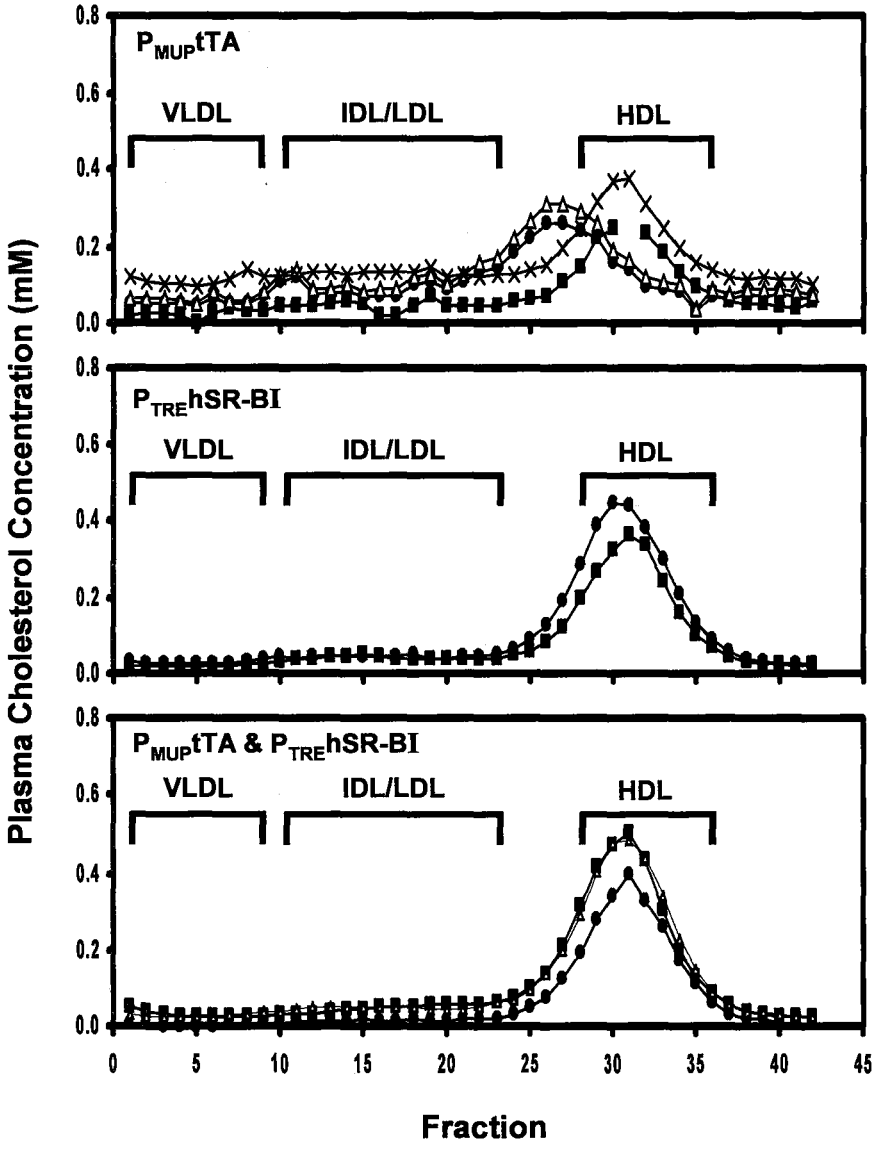


**Figure 15. Lipoprotein cholesterol profiles of fasted $P_{MUP}$tTA / $P_{TRE}$hSR-BI double transgenic and control mice.** Plasma samples from overnight fasted 10 week old $P_{MUP}$-tTA (A) and $P_{TRE}$hSR-BI (B) single transgenic control mice and from $P_{MUP}$tTA / $P_{TRE}$hSR-BI double transgenic mice (C) were size fractionated using Superose 6 10/30 GL gel filtration column on an AKTA FPLC. Fractions (42) beginning at the void volume were collected and total cholesterol was assayed. The fractions were assayed for total cholesterol. Plasma lipoprotein cholesterol profiles were not altered in $P_{MUP}$tTA / $P_{TRE}$hSR-BI (line 268) double transgenic mice.

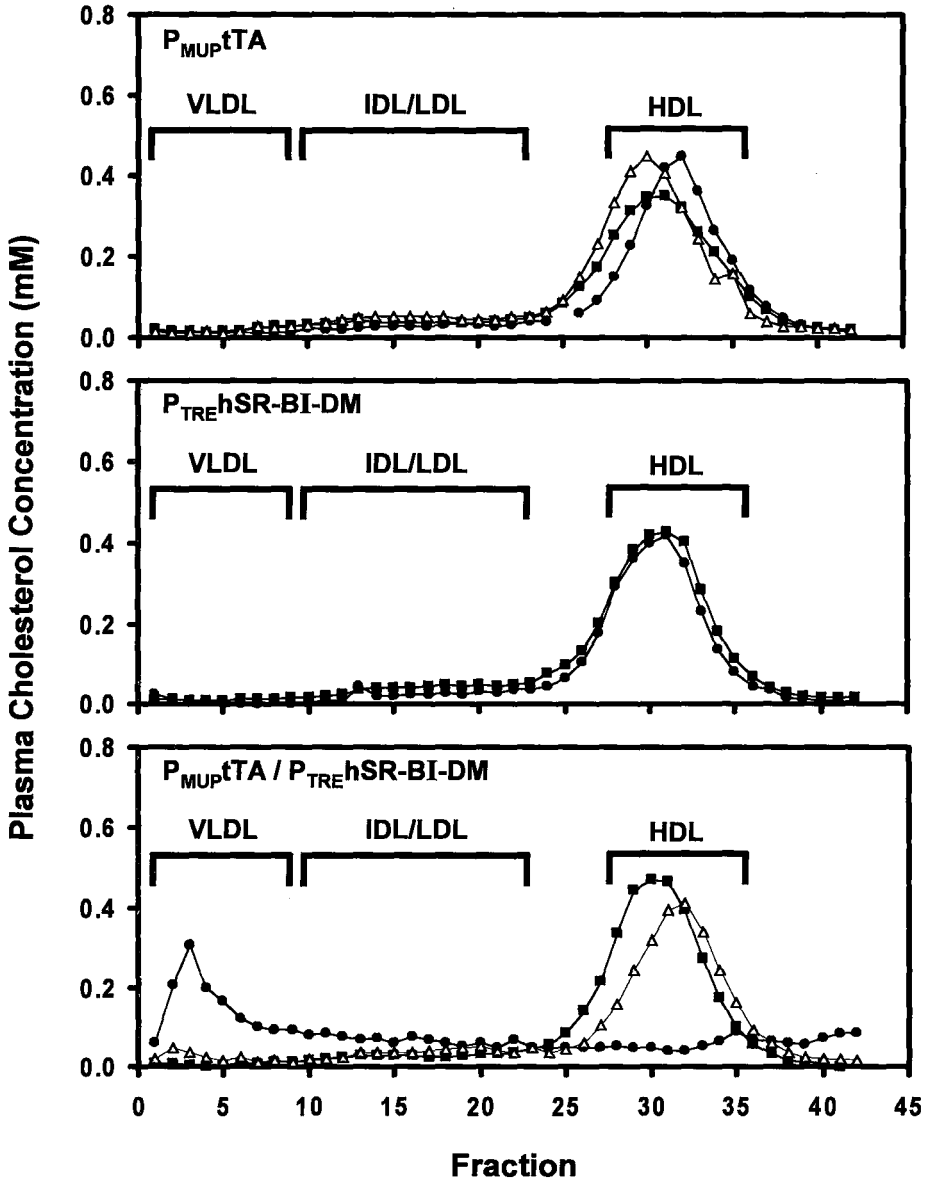


**Figure 16. Lipoprotein cholesterol profiles of fasted $P_{MUP}$tTA / $P_{TRE}$hSR-BI-DM double transgenic and control mice.** Plasma samples from overnight fasted 10 week old $P_{MUP}$-tTA (A) and $P_{TRE}$hSR-BI (B) single transgenic control mice and from $P_{MUP}$tTA / $P_{TRE}$hSR-BI double transgenic mice (C) were size fractionated using Superose 6 10/30 GL gel filtration column on an AKTA FPLC. Fractions (42) beginning at the void volume were collected and total cholesterol was assayed. The fractions were assayed for total cholesterol. Plasma lipoprotein cholesterol profiles were not altered in $P_{MUP}$tTA / $P_{TRE}$hSR-BI-DM (line 4766) double transgenic mice.

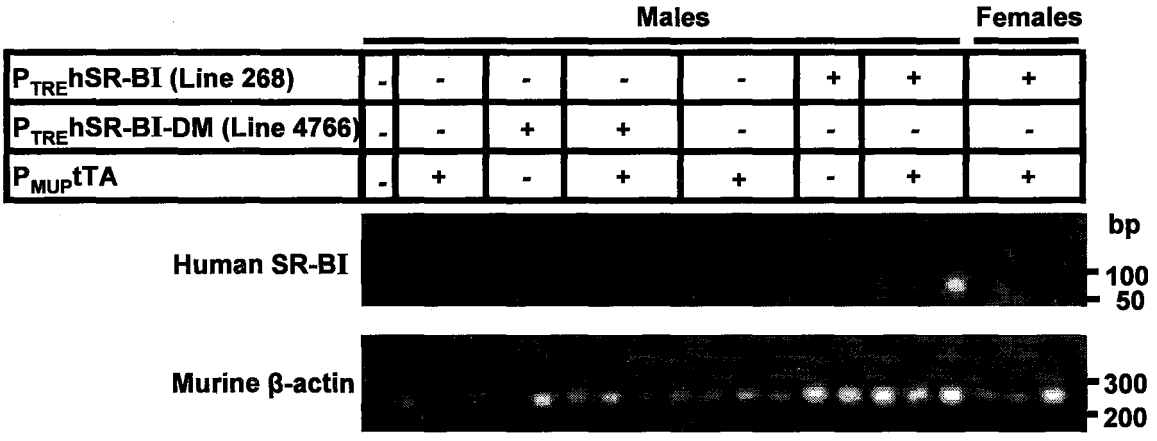


**Figure 17. RT-PCR detection of hSR-BI transcripts in the livers of $P_{MUP}$tTA / $P_{TRE}$hSR-BI double transgenic mice.** RNA was prepared from livers of $P_{MUP}$tTA / $P_{TRE}$hSR-BI and $P_{MUP}$tTA / $P_{TRE}$hSR-BI-DM double transgenic mice, as well as from $P_{MUP}$tTA and $P_{TRE}$hSR-BI or $P_{TRE}$hSR-BI-DM, respectively, single transgenic control mice. cDNA was synthesized and used as the template in PCR reactions to detect the presence of either hSR-BI or hSR-BI-DM mRNA transcripts. Primers were designed so as not to detect mSR-BI mRNA transcripts or genomic DNA. If mSR-BI genomic DNA were amplified a 1051 bp product would be obtained. PCR reactions were also run to amplify murine β-actin transcripts in order to control for varying concentrations of cDNA in the samples. $P_{MUP}$tTA / $P_{TRE}$hSR-BI (line 268) double transgenic mice have hSR-BI mRNA transcripts in their livers, suggesting that hSR-BI transgene is expressed in $P_{MUP}$tTA / $P_{TRE}$hSR-BI (line 268) livers.

expression of hSR-BI or hSR-BI-DM, respectively and β-galactosidase in the liver of $P_{MUP}$tTA / $P_{TRE}$hSR-BI (line 268) and $P_{MUP}$tTA / $P_{TRE}$hSR-BI-DM (line 4766) mice were compared to those of single transgenic control mice. Liver lysates from the mice were subjected to SDS-PAGE and transferred to PVDF membranes (refer to B.2. Methods). Immunoblotting for hSR-BI and hSR-BI-DM was conducted using antibodies raised against the C-terminus and the extracellular loop of the protein, respectively (refer to B.2. Methods). No differences in SR-BI protein levels were detected in lysates of $P_{MUP}$tTA / $P_{TRE}$hSR-BI double transgenic mice (Fig 18A). Similarly, no specific band corresponding to hSR-BI-DM was detected in liver lysates from $P_{MUP}$tTA / $P_{TRE}$hSR-BI-DM (line 4766) double transgenic mouse (Fig 18B). A band of the expected size was detected in the liver lysate from one $P_{MUP}$tTA / $P_{TRE}$hSR-BI-DM (line 4766) double transgenic (Fig 18B lane 8) and one $P_{TRE}$hSR-BI-DM (line 4766) single transgenic mouse (Fig 18B lane 6) but likely represented a non-specific band since it was not detected in the liver lysates from other $P_{MUP}$tTA / $P_{TRE}$hSR-BI-DM (line 4766) double transgenic mice (Fig 18B lanes 9-11). Immunoblots for β-galactosidase (refer to B.2. Methods) show that all $P_{MUP}$tTA / $P_{TRE}$hSR-BI (line 268) and $P_{MUP}$tTA / $P_{TRE}$hSR-BI-DM (line 4766) double transgenic mice expressed the enzyme in their livers (Fig 18A & B). Immunoblotting for ε-COP (Fig 18A) and β-actin (Fig 18B) are shown as loading controls. Immunoblotting for β-actin was also performed on the β-galactosidase blot shown in Fig 18A; however, the data is not shown.

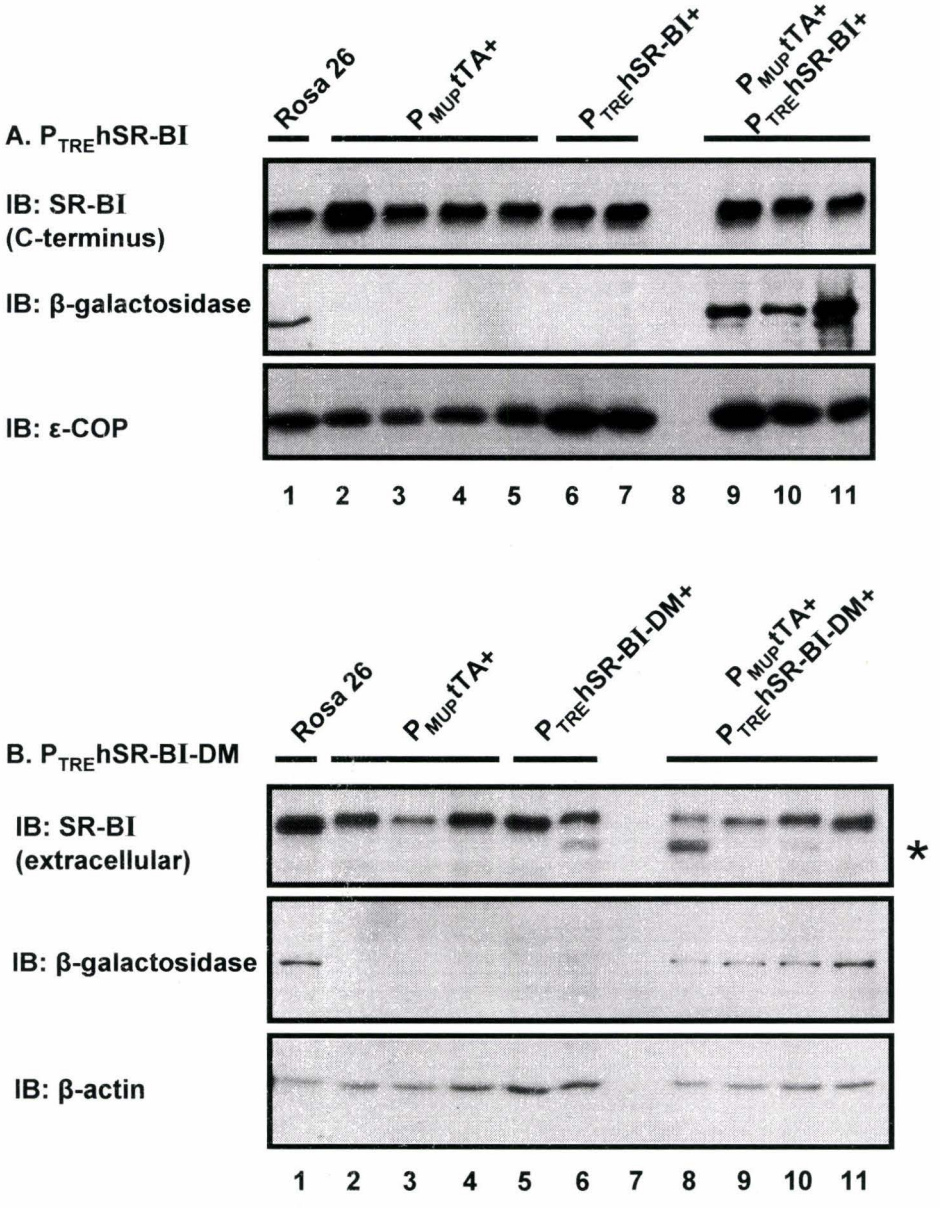
A. P TRE hSR-BI
Rosa 26
P MUP tTA+
P TRE hSR-BI+
P MUP tTA+ P TRE hSR-BI+
IB: SR-BI (C-terminus)
IB: β-galactosidase
IB: ε-COP
1 2 3 4 5 6 7 8 9 10 11
B. P TRE hSR-BI-DM
Rosa 26
P MUP tTA+
P TRE hSR-BI-DM+
P MUP tTA+ P TRE hSR-BI-DM+
IB: SR-BI (extracellular)
*
IB: β-galactosidase
IB: β-actin
1 2 3 4 5 6 7 8 9 10 11

**Figure 18. Immnunoblot analysis of SR-BI and β-galactosidase in livers of $P_{MUP}$-tTA / $P_{TRE}$-hSR-BI and $P_{MUP}$-tTA / $P_{TRE}$-hSR-BI-DM double transgenic mice and control mice.** Liver homogenates prepared from 10 week old $P_{MUP}$-tTA / $P_{TRE}$-hSR-BI (A) and $P_{MUP}$-tTA / $P_{TRE}$-hSR-BI-DM (B) double transgenic mice, as well as from $P_{MUP}$-tTA (A & B) and $P_{TRE}$-hSR-BI (A) or $P_{TRE}$-hSR-BI-DM (B) single transgenic control mice, were subjected to SDS-PAGE. All mice were males. Immunoblotting was performed: For SR-BI (top panels in A and B), using the antibodies raised against (A) SR-BI's C-terminus to detect full length hSR-BI or (B) SR-BI's extracellular region to detect hSR-BI-DM (which lacks the C-terminal cytoplasmic region); for β-galactosidase (middle panels of A and B); and for either ε-COP (bottom panel of A) or β-actin (bottom panel of B), both used as loading conrols. The asterix in B denotes a non-specific band. No increases in hSR-BI or hSR-BI-DM protein expression were detected in the livers of the double transgenic mice (lanes 9-11 in A, and 8-11 in B), compared to the single transgenic controls, suggesting that steady state levels of hSR-BI and hSR-BI-DM proteins were below the level of detection.

To verify that hSR-BI was not being expressed in various other tissues in the $P_{MUP}$tTA / $P_{TRE}$hSR-BI (line 268) double transgenic mice, tissue lysates from mice of this genotype, as well as from single transgenic controls, were subjected to SDS-PAGE and immunoblotting for SR-BI (Fig 19A). No increases in SR-BI expression were detected in lysates of adipose tissue, brain, heart, intestine, kidney, lung, skeletal muscle, spleen and stomach lysates of the double transgenic mice compared to $P_{MUP}$tTA or $P_{TRE}$hSR-BI (line 268) single transgenic control mice. Adrenal gland lysates were analyzed separately due to the very high levels of endogenous SR-BI expression in this tissue. No differences in SR-BI expression were detected in adrenal glands from $P_{MUP}$tTA / $P_{TRE}$hSR-BI (line 268) or $P_{MUP}$tTA / $P_{TRE}$hSR-BI-DM (line 4766) double transgenic mice and corresponding single transgenic mice (Fig 19B). Therefore, although the promoter was active specifically in the liver, as demonstrated by the liver-specific β-galactosidase activity and the detection of hSR-BI sequences by RT-PCR, $P_{MUP}$tTA / $P_{TRE}$hSR-BI (line 268) and $P_{MUP}$tTA / $P_{TRE}$hSR-BI-DM (line 4766) double transgenic mice did not appear to express hSR-BI or hSR-BI-DM proteins, respectively.

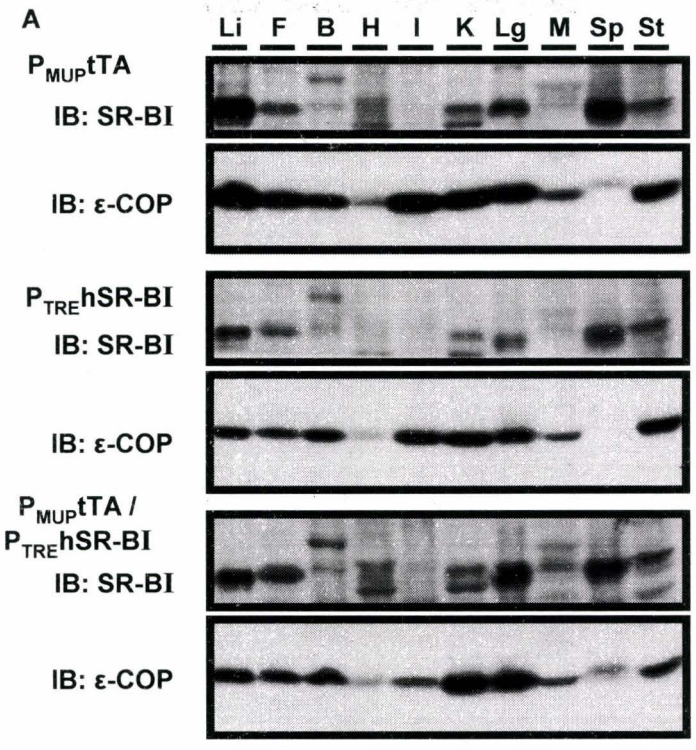
A
Li F B H I K Lg M Sp St
$P_{MUP}$tTA
IB: SR-BI
IB: ε-COP
$P_{TRE}$hSR-BI
IB: SR-BI
IB: ε-COP
$P_{MUP}$tTA /
$P_{TRE}$hSR-BI
IB: SR-BI
IB: ε-COP

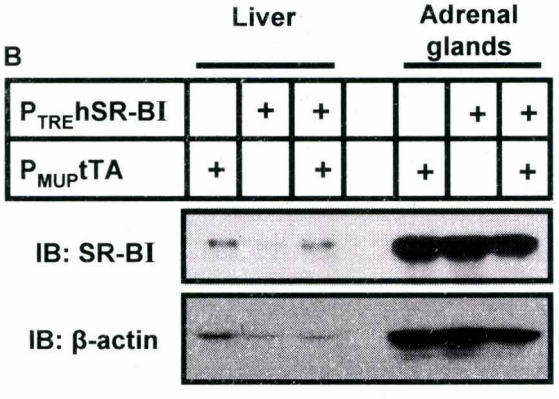
B
Liver
Adrenal glands
$P_{TRE}$hSR-BI
$P_{MUP}$tTA
IB: SR-BI
IB: β-actin

**Figure 19. Immnunoblot analysis of SR-BI in various tissues of $P_{MUP}$-tTA / $P_{TRE}$-hSR-BI and $P_{MUP}$-tTA / $P_{TRE}$-hSR-BI-DM double transgenic mice and control mice.** **Panel A:** Liver (Li), adipose (F), brain (B), heart (H), intestine (I), kidney (K), lung (L), skeletal muscle (M), spleen (Sp) and stomach (St) tissues were harvested from $P_{MUP}$-tTA / $P_{TRE}$-hSR-BI double transgenic and single transgenic controls as indicated. Tissues were homogenized and proteins (30 μg/lane) were subjected to SDS-PAGE and immunoblotting for SR-BI (using the antibody directed against SR-BI's C terminus) or for ε-COP as a loading control. **Panel B:** Homogenates of livers and adrenal glands from the same mice as those in A were subjected to SDS-PAGE (30 μg/lane) and immunoblotting for SR-BI (as in panel A) or β-actin as a loading control, as indicated. No increases in SR-BI protein levels were detected in any of the tissues of $P_{MUP}$tTA / $P_{TRE}$hSR-BI double transgenic mice, compared to the single transgenic controls

# D. Discussion

## D.1. Effects of the C-terminal Cytoplasmic Tail of Human SR-BI on the Localization, Function and Regulation of the Protein

Hepatic SR-BI has previously been shown to mediate the selective uptake of cholesterol esters and free cholesterol from HDL particles (Ji et al. 1999; Silver et al. 2001; Brundert et al. 2005; Shetty et al. 2006; Sun et al. 2006) and to play an important role in mice in the protection against atherosclerosis by mediating HDL cholesterol clearance from blood by the liver, driving RCT (Kozarsky et al. 1997; Varban et al. 1998; Wang et al. 1998; Arai et al. 1999; Ueda et al. 1999; Huszar et al. 2000; Kozarsky et al. 2000; Ueda et al. 2000; Huby et al. 2006). As well, the last 3 amino acids of the C-terminal tail of SR-BI are required for interaction with PDZK1, an adaptor protein which modulates SR-BI's steady-state levels in the liver (Ikemoto et al. 2000; Silver 2002; Yesilaltay et al. 2006). PDZK1 knockout mice have a 95% reduction in hepatic SR-BI steady-state levels and an increase in plasma cholesterol levels similar to that of SR-BI knockout mice (Kocher 2003). Additionally, in endothelial cells the C-terminal tail of SR-BI is required for the activation of various processes which protect against atherosclerosis (Yuhanna et al. 2001; Kimura et al. 2006). These results indicate that the C-terminal tail of SR-BI may play an important role in the protein's atheroprotective functions. In order to further characterize this region of the protein, the effects of deleting the C-terminal tail of SR-BI on the protein's localization in hepatocytes and endothelial cells, as well as its function and regulation in hepatocytes was determined.

Imaging of HepG2 cells expressing EGFP or MRFP tagged hSR-BI (full length or C-terminal deletion mutant) demonstrated that these proteins were localized to the cell periphery as well as to juxtanuclear punctate structures. The distribution was not affected by deletion of the C-terminal tail. Previous studies have also shown that full length SR-BI was localized to the plasma membrane of hepatocytes (Landschulz et al. 1996; Kozarsky et al. 1997; Hatzopoulos et al. 1998; Ikemoto et al. 2000; Silver et al. 2001; Sehayek et al. 2003; Rhainds et al. 2004; Nakagawa-Toyama et al. 2005; Harder et al. 2007). In addition, the data is consistent with findings reported by others that SR-BI is found on the cell surface as well as in ERC (Rigotti et al. 1997; Silver et al. 2001).

In primary human and murine aortic endothelial cells EGFP-hSR-BI was distributed in a punctate pattern. As observed in HepG2 cells, there were no differences between the localization of the EGFP-tagged full length and C-terminal truncation mutant SR-BI proteins in HAEC or MAEC. Similarly, the localization of EGFP-tagged *murine* SR-BI was unaltered by the removal of its C-terminal tail in CHO cells (Eckhardt et al. 2004). It is not clear if this punctate distribution represents localization in ERC as in other cell types such as hepatocytes, CHO cells and MDCK cells (Babitt et al. 1997; Silver et al. 2001; Burgos et al. 2004). In contrast, Yeh and collaborators found that SR-BI localized to the cell surface of endothelial cells in rat aortas (Yeh et al. 2002). The difference in distribution may reflect the cell culture system versus intact tissues and/or effects of overexpression. Further work is required too address this issue.

Functional characterization of EGFP-hSR-BI-DM, by means of DiI-HDL lipid uptake assay, revealed that deletion of hSR-BI's C-terminal tail reduced the specific activity of SR-BI in HDL-lipid uptake by 50%. This suggested that although the C-terminal tail was not absolutely required for activity, in agreement with a previous study demonstrating that the extracellular loop, but not the C-terminal cytoplasmic domain of *murine* SR-BI is required for HDL CE selective uptake, it did influence the level of activity (Gu et al. 1998; Connelly et al. 2001). Recent reports have shown that the C-terminal tail of SR-BI may be implicated in the protein's dimerization (Sahoo, Peng et al.), Perhaps, the effects of the C-terminal truncation mutant on oligomerization results in the reduced HDL-lipid uptake activity.

Characterization of the regulation of hSR-BI mediated HDL-lipid uptake, conducted by determining the effects of PMA or calphostin C treatments on DiI-HDL lipid uptake in HepG2 cells stably overexpressing EGFP-hSR-BI, demonstrated that activity is regulated by PKC. Although these results mirror data showing that HDL-lipid uptake activity in ldlA[*m*SR-BI] and HepG2 cells is also decreased by PKC inhibition, they differ from data which showed that in ldlA[*h*SR-BI] cells PKC does not regulate HDL-lipid uptake (Witt et al. 2000; Zhang et al. b 2007). Perhaps regulation of *human* SR-BI's HDL-lipid uptake activity by the PKC signalling pathway varies between cell types. Calphostin C treatment also decreased HDL-lipid uptake in HepG2 cells overexpressing EGFP-hSR-BI-DM; however, no statistically significant increase in HDL-lipid uptake activity was observed when these cells were treated with PMA. These

results indicate that the C-terminus of SR-BI is not required for the decrease in HDL-lipid uptake activity of the protein caused by calphostin C inhibition of PKC.

In addition, BLT-1 reduced HDL-lipid uptake in HepG2 cells overexpressing EGFP-hSR-BI or EGFP-hSR-BI-DM by ~20 or 25%, respectively. This level of inhibition is much less than that reported for the HDL-lipid uptake in CHO derived cells overexpressing *murine* SR-BI (Nieland et al. 2002). Further research is required to determine if this apparent difference in the potency of BLT-1 is the result of interspecies variations between human SR-BI (this study) and mSR-BI proteins (Nieland et al. 2002).

### D.2. Analysis of $P_{MUP}$tTA / $P_{TRE}$hSR-BI and $P_{MUP}$tTA / $P_{TRE}$hSR-BI-DM Transgenic Mice

To investigate the *in vivo* function of human SR-BI and the effects of the deletion of the C-terminal cytoplasmic domain, I attempted to generate liver specific hSR-BI and hSR-BI-DM transgenic mice. A bipartite tetracycline expression system, requiring mice expressing driver, $P_{MUP}$tTA, and responder, $P_{TRE}$hSR-BI or $P_{TRE}$hSR-BI-DM, transgenes, was used to generate liver-specific hSR-BI or hSR-BI-DM transgenic mice, respectively. In double transgenic mice generated from one transgenic line each for $P_{TRE}$hSR-BI and $P_{TRE}$hSR-BI-DM, liver restricted β-galactosidase protein and enzyme activity was detected in males. This is consistent with reports that MUP expression is regulated by testosterone and is at least 5-fold greater in males than in females (Hastie et al. 1979). Transcripts of hSR-BI-DM were not detected in the livers of $P_{MUP}$tTA / $P_{TRE}$hSR-BI-DM

double transgenic mice. Perhaps further optimization of the RT-PCR conditions for the hSR-BI-DM transcripts are required since low levels of β-galactosidase activity indicate that the livers of these mice would have low transcript levels. On the other hand, hSR-BI transcripts were detected in the livers of $P_{MUP}$tTA / $P_{TRE}$hSR-BI double transgenic mice, but these were accompanied neither by increased SR-BI protein nor by altered plasma lipoprotein cholesterol. Hepatic overexpression of human SR-BI is expected to increase hepatic HDL clearance, thereby reducing plasma HDL cholesterol levels based on studies of hepatic overexpression of mSR-BI in mice or hSR-BI in rabbits (Kozarsky et al. 1997; Wang et al. 1998; Arai et al. 1999; Ueda et al. 2000; Tancevski et al. 2005). These results indicate that in the $P_{MUP}$tTA / $P_{TRE}$hSR-BI double transgenic mice either hSR-BI protein translation or stability is reduced. A recent report has indicated that PDZK1 acts in a species specific manner: that murine PDZK1 does not bind to or prevent human SR-BI from being degraded (Komori et al. 2006). If this is the case, co-expression of human PDZK1 may be a way to overcome the lack of an increase in SR-BI protein. Further research is required to test this.

## E. Conclusion

In this study I examined the localization, activity and regulation of full length and C-terminal truncation mutant hSR-BI. EGFP-tagged hSR-BI and hSR-BI-DM proteins localized in punctate patterns within HAEC and WT or SR-BI null MAEC. In addition, similar localization patterns were observed in HepG2 cells; however, in these cells the proteins were also expressed in juxtanuclear regions and at the cell periphery. Expression of EGFP-hSR-BI and MRFP-hSR-BI-DM or MRFP-hSR-BI and EGFP-hSR-BI-DM in HepG2 cells revealed that the full length and truncation mutant hSR-BI proteins colocalize. This indicated that deletion of the C-terminus of the protein did not affect its localization. The C-terminal truncation mutant hSR-BI mediated HDL-lipid uptake in HepG2 cells, but to a lesser extent than hSR-BI. In addition, in HepG2 cells hSR-BI and hSR-BI-DM-mediated HDL-lipid uptake activity was decreased by calphostin C. Based on these findings, hSR-BI may be regulated by PKC in a manner that is independent of its C-terminal tail.

To study the effects of human SR-BI and its C-terminal tail *in vivo*, we set out to generate transgenic mice with liver-specific overexpression of hSR-BI or hSR-BI-DM using a bipartite expression system. Responder transgenic mice expressing $P_{TRE}$hSR-BI or $P_{TRE}$hSR-BI-DM were generated and mated to driver mice, $P_{MUP}$tTA. The resulting double transgenic and single transgenic mice showed that liver-specific expression of the β-galactosidase reporter was attained. However, mRNA transcripts

for hSR-BI, but not for hSR-BI-DM were detected in the livers of $P_{MUP}$tTA / $P_{TRE}$hSR-BI and $P_{MUP}$tTA / $P_{TRE}$hSR-BI-DM mice, respectively. Despite these results, neither hSR-BI nor hSR-BI-DM proteins were expressed in the livers of the $P_{MUP}$tTA / $P_{TRE}$hSR-BI and $P_{MUP}$tTA / $P_{TRE}$hSR-BI-DM mice, respectively.

## F. Bibliography

Acton, S., A. Rigotti, K. T. Landschulz, S. Xu, H. H. Hobbs and M. Krieger (1996) Identification of scavenger receptor SR-BI as a high density lipoprotein receptor. *Science* **271,** 518-520.

Acton, S. L., P. E. Scherer, H. F. Lodish and M. Krieger (1994) Expression cloning of SR-BI, a CD36-related class B scavenger receptor. *J Biol Chem* **269,** 21003-21009.

Arai, T., N. Wang, M. Bezouevski, C. Welch and A. R. Tall (1999) Decreased atherosclerosis in heterozygous low density lipoprotein receptor-deficient mice expressing the scavenger receptor BI transgene. *J Biol Chem* **274,** 2366-2371.

Babitt, J., B. Trigatti, A. Rigotti, E. J. Smart, R. G. Anderson, S. Xu and M. Krieger (1997) Murine SR-BI, a high density lipoprotein receptor that mediates selective lipid uptake, is N-glycosylated and fatty acylated and colocalizes with plasma membrane caveolae. *J Biol Chem* **272,** 13242-13249.

Brown, M. S. and J. L. Goldstein (1986) A receptor-mediated pathway for cholesterol homeostasis. *Science* **232,** 34-47.

Brundert, M., A. Ewert, J. Heeren, B. Behrendt, R. Ramakrshnan, H. Greten, M. Merkel and F. Rinninger (2005) Scavenger Receptor Class B Type I Mediates the Selective Uptake of High-Density Lipoprotein–Associated Cholesteryl Ester by the Liver in Mice. *Arterioscler Thromb Vasc Biol* **25,** 143-148.

Burgos, P. V., C. Klattenhoff, E. de la Fuente, A. Rigotti and A. Gonzalez (2004) Cholesterol depletion induces PKA-mediated basolateral-to-apical transcytosis of the scavenger receptor class B type I in MDCK cells. *Proc Natl Acad Sci U S A* **101,** 3845-3850.

Cai, S. F., K. R. J., P. N. Howles and D. Y. Hui (2001) Differentiation-dependent expression and localization of the class B type I scavenger receptor in intestine. *J Lip Res* **42.**

Calvo, D., D. Gomez-Coronado, M. A. Lasuncion and M. A. Vega (1997) CLA-1 is an 85-kD plasma membrane glycoprotein that acts as a high-affinity receptor for both native (HDL, LDL, and VLDL) and modified (OxLDL and AcLDL) lipoproteins. *Arterioscler Thromb Vasc Biol* **17,** 2341-2349.

Cao, W. M., K. Murao, H. Imachi, X. Yu, H. Abe, A. Yamauchi, M. Niimi, A. Miyauchi, N. C. Wong and T. Ishida (2004) A mutant high-density lipoprotein receptor inhibits proliferation of human breast cancer cells. *Cancer Res* **64,** 1515-1521.

Chapman, M. J., S. Goldstein, D. Lagrange and P. M. Laplaud (1981) A density gradient ultracentrifugation procedure for isolation of major lipoprrptein classes from human serum. *J Lip Res* **22,** 339-358

Connelly, M. A., M. de la Llera-Moya, P. Monzo, P. G. Yancey, D. Drazul, G. Stoudt, N. Fournier, S. M. Klein, G. H. Rothblat and D. L. Williams (2001) Analysis of chemeric receptors shows that multiple distinct functional activities of scavenger receptor, class B type I (SR-BI), are localized to the extracellular receptor domain. *Biochemistry* **40,** 5249-5259.

Covey, S. D., M. Krieger, W. Wang, M. Penman and B. L. Trigatti (2003) Scavenger receptor class B type I-mediated protection against atherosclerosis in LDL receptor-negative mice involves its expression in bone marrowderived cells. *Arterioscler Thromb Vasc Biol* **23,** 1589–1594.

Eckhardt, E. R., L. Cai, B. Sun, N. R. Webb and D. R. van der Westhuyzen (2004) High density lipoprotein uptake by scavenger receptor SR-BII. *J Biol Chem* **279,** 14372-14381.

Fuster, V., L. Badimon, J. J. Badimon and J. H. Chesebro (1992) The pathogenesis of coronary artery disease and the acute coronary syndromes (2). *N Engl J Med* **326,** 310-318.

Gillotte-Taylor, K., A. Boullier, J. L. Witztum, D. Steinberg and O. Quehenberger (2001) Scavenger receptor class B type I as a receptor for oxidized low density lipoprotein. *J Lipid Res* **42,** 1474-1482.

Glass, C., R. C. Pittman, D. B. Weinstein and D. Steinberg (1983) Dissociation of tissue uptake of cholesterol ester from that of apoprotein A-I of rat plasma high density lipoprotein: selective delivery of cholesterol ester to liver, adrenal, and gonad. *Proc Natl Acad Sci U S A* **80,** 5435-5439.

Glomset, J. A. (1968) The plasma lecithins:cholesterol acyltransferase reaction. *J Lipid Res* **9,** 155-167.

Gordon, D. J. and B. M. Rifkind (1989) High-density lipoprotein--the clinical implications of recent studies. *N Engl J Med* **321,** 1311-1316.

Gosling, J., S. Slaymaker, L. Gu, S. Tseng, C. H. Zlot, S. G. Young, B. J. Rollins and I. F. Charo (1999) MCP-1 deficiency reduces susceptibility to atherosclerosis in mice that overexpress human apolipoprotein B. *J Clin Invest* **103,** 773-778.

Gossen, M. and H. Bujard (1992) Tight control of gene expression in mammalian cells by tetracycline-responsive promoters. *Proc Natl Acad Sci U S A* **89,** 5547-5551.

Grewal, T., I. de Diego, M. F. Kirchhoff, F. Tebar, J. Heeren, F. Rinninger and C. Enrich (2003) High density lipoprotein-induced signaling of the MAPK pathway involves scavenger receptor type BI-mediated activation of Ras. *J Biol Chem* **278,** 16478-16481.

Gu, X., R. Lawrence and M. Krieger (2000) Dissociation of the high density lipoprotein and low density lipoprotein binding activities of murine scavenger receptor class B type I (mSR-BI) using retrovirus library-based activity dissection. *J Biol Chem* **275,** 9120-9130.

Gu, X., B. Trigatti, S. Xu, S. Acton, J. Babitt and M. Krieger (1998) The efficient cellular uptake of high density lipoprotein lipids via scavenger receptor class B type I requires not only receptor-mediated surface binding but also receptor-specific lipid transfer mediated by its extracellular domain. *J Biol Chem* **273,** 26338-26348.

Hansson, G. K., P. Libby, U. Schonbeck and Z. Q. Yan (2002) Innate and adaptive immunity in the pathogenesis of atherosclerosis. *Circ Res* **91,** 281-291.

Harder, C. J., A. Meng, P. Rippstein, H. M. McBride and R. McPherson (2007) SR-BI Undergoes Cholesterol-stimulated Transcytosis to the Bile Canaliculus in Polarized WIF-B Cells. *J. Biol Chem* **282,** 1445-1455.

Harder, C. J., G. Vassiliou, H. M. McBride and R. McPherson (2006) Hepatic SR-BI-mediated cholesteryl ester selective uptake occurs with unaltered efficiency in the absence of cellular energy. *J Lip Res* **47,** 492503.

Hartung, D. and J. Narula (2004) Targeting the inflammatory component in atherosclerotic lesions vulnerable to rupture. *Z Kardiol* **93,** 97-102.

Hastie, N. D., W. A. Held and J. J. Toole (1979) Multiple genes coding for the androgen-regulated major urinary proteins of the mouse. *Cell* **17,** 449-457.

Hatzopoulos, A. K., A. Ribotti, R. D. Rosenberg and M. Krieger (1998) Temporal and spatial pattern of expression of the HDL receptor SR-BI during murine embryogenesis. *J Lip Res* **39,** 495-508.

Huby, T., C. Doucet, C. Dachet, B. Ouzilleau, Y. Ueda, V. Afzal, E. Rubin, M. J. Chapman and P. Lesnik (2006) Knockdown expression and hepatic deficiency reveal an atheroprotective role for SR-BI in liver and peripheral tissues. *J. Clin Invest* **116,** 2767-2776.

Huszar, D., M. L. Varban, F. Rinninger, R. Feeley, T. Arai, V. Fairchild-Huntress, M. J. Donovan and A. R. Tall (2000) Increased LDL cholesterol and atherosclerosis in LDL receptor-deficient mice with attenuated expression of scavenger receptor B1. *Arterioscler Thromb Vasc Biol* **20,** 1068-1073.

Ihrke, G., E. B. Neufeld, T. Meads, M. R. Shanks, D. Cassio, M. Laurent, T. A. Schroer, R. E. Pagano and A. L. Hubbard (1993) WIF-B Cells: an in vitro model for studies of hepatocyte polarity. *Journal of Cell Biology* **123,** 1761-1775.

Ikemoto, M., H. Arai, D. Feng, K. Tanaka, J. Aoki, N. Dohmae, K. Takio, H. Adachi, M. Tsujimoto and K. Inoue (2000) Identification of a PDZ-domain-containing protein that interacts with the scavenger receptor class B type I. *Proc. Natl. Acad. Sci. U. S. A.* **97,** 6538-6543.

Jang, M. K., J. Y. Kim, N. H. Jeoung, M. A. Kang, M. S. Choi, G. T. Oh, K. T. Nam, W. H. Lee and Y. B. Park (2004) Oxidized low-density lipoproteins may induce expression of monocyte chemotactic protein-3 in atherosclerotic plaques. *Biochem Biophys Res Commun* **323,** 898-905.

Jessup, W., L. Kritharides and R. Stocker (2004) Lipid oxidation in atherogenesis: an overview. *Biochem Soc Trans* **32,** 134-138.

Ji, Y., N. Wang, R. Ramakrishnan, E. Sehayek, D. Huszari, J. L. Breslow and A. R. Tall (1999) Hepatic scavenger receptor BI promotes rapid clearance of high density lipoprotein free cholesterol and its transport into bile. *J Biol Chem* **274,** 33398-33402.

Kawamura, T., A. Furusaka, M. J. Koziel, R. T. Chung, T. C. Wang, E. V. Schmidt and T. J. Liang (1997) Transgenic expression of hepatitic C virus structural proteins in mice. *Hepatology* **25,** 1014-1021.

Kimura, T., H. Tomura, C. Mogi, A. Kuwabara, A. Damirin, T. Ishizuka, A. Sekiguchi, M. Ishiwara, D. Im, K. Sato, M. Murakami and F. Okajima (2006) Role of scavenger receptor class B type I and spingosine 1- phosphate receptor molecules in high density lipoprotein-induced inhibition of adhesion molecule expression in endothelial cells. *J. Biol Chem* **281,** 37457-37467.

Kocher, O., N. Comella, K. Tognazzi and L. F. Brown (1998) Identification and partial characterization of PDZK1: a novel protein containing PDZ interaction domains. *Lab Invest* **78,** 117-125.

Kocher, O., Pal, R., Roberts, M., Cirovic, C., Gilchrist, A. (2003) Targeted disruption of the PDZK1 gene by homologous recombination. *Mol Cell Biol* **23,** 1175-1180.

Komori, H., T. Kita and Y. Ueda (2006). Human PDZK1 expression enhanced the human SR-BI (CLA-1) expression in the liver of CLA-1 transgenic mouse, American Heart Association.

Kozarsky, K. F., M. H. Donahee, J. M. Glick, M. Krieger and D. J. Rader (2000) Gene transfer and hepatic overexpression of the HDL receptor SR-BI reduces atherosclerosis in

the cholesterol-fed LDL receptor-deficient mouse. *Arterioscler Thromb Vasc Biol* **20,** 721-727.

Kozarsky, K. F., M. H. Donahee, A. Ribotti, S. N. Iqbal, E. R. Edelman and M. Krieger (1997) Overexpression of the HDL receptor SR-BI alters plasma HDL and bile cholesterol levels. *Nature* **387,** 414–417.

Krieger, M. (1998) The "best" of cholesterols, the "worst" of cholesterols: a tale of two receptors. *Proc Natl Acad Sci U S A* **95,** 4077-4080.

Krieger, M. (2001) Scavenger receptor class B type I is a multiligand HDL receptor that influences diverse physiologic systems. *J Clin Invest* **108,** 793-797.

Kume, N., M. I. Cybulsky and M. A. Gimbrone, Jr. (1992) Lysophosphatidylcholine, a component of atherogenic lipoproteins, induces mononuclear leukocyte adhesion molecules in cultured human and rabbit arterial endothelial cells. *J Clin Invest* **90,** 1138-1144.

Laemmli, U. K. (1970) Cleavage of structural proteins during the assembly of the head of bacteriophage T4. *Nature* **227,** 680-685.

Lamarche, B. and G. F. Lewis (1998) Atherosclerosis prevention for the next decade: risk assessment beyond low density lipoprotein cholesterol. *Can J Cardiol* **14,** 841-851.

Landschulz, K. T. P., R. K., A. Rigotti, M. Krieger and H. H. Hobbs (1996) Regulation of scavenger receptor, class B, type I, a high density lipoprotein receptor, in liver and steroidogenic tissues of the rat. *J. Clin. Invest.* **98,** 984-995.

Li, X., Guo, L., Dressman, J. L., Asmis, R., Smart, E. J. (2005) A Novel Ligand-independent Apoptotic Pathway Induced by Scavenger Receptor Class B, Type I and Suppressed by Endothelial Nitric-oxide Synthase and High Density Lipoprotein. *J Biol Chem* **280,** 19087-19096.

Li, X. A., W. B. Titlow, B. A. Jackson, N. Giltiay, M. Nikolova-Karakashian, A. Uittenbogaard and E. J. Smart (2002) High density lipoprotein binding to scavenger receptor, Class B, type I activates endothelial nitric-oxide synthase in a ceramide-dependent manner. *J Biol Chem* **277,** 11058-11063.

Liadaki, K. N., T. Liu, S. Xu, B. Y. Ishida, P. N. Duchateaux, J. P. Krieger, J. Kane, M. Krieger and V. I. Zannis (2000) Binding of high density lipoprotein (HDL) and discoidal reconstituted HDL to the HDL receptor scavenger receptor class B type I. Effect of lipid association and APOA-I mutations on receptor binding. *J Biol Chem* **275,** 21262-21271.

Libby, P., P. M. Ridker and A. Maseri (2002) Inflammation and atherosclerosis. *Circulation* **105,** 1135-1143.

Linton, M. F. and S. Fazio (2003) Macrophages, inflammation, and atherosclerosis. *Int J Obes Relat Metab Disord* **27 Suppl 3,** S35-40.

Martin, J. E., A. Lester, D. S. Kellogg and J. D. Thayer (1969) In vitro susceptibility of Neisseria gonorrhoeae to nine antimicrobial agents. *Applied Microbiology* **18,** 21-23.

Mendez, A. J. (1997) Cholesterol efflux mediated by apolipoproteins is an active cellular process distinct from efflux mediated by passive diffusion. *J Lipid Res* **38,** 1807-1821.

Mineo, C. and P. W. Shaul (2003) HDL stimulation of endothelial nitric oxide synthase: a novel mechanism of HDL action. *Trends in Cardivascular Medicine* **13,** 226-231.

Mineo, C., I. S. Yuhanna, M. J. Quon and P. W. Shaul (2003) High density lipoprotein-induced endothelial nitric-oxide synthase activation is mediated by Akt and MAP kinases. *J Biol Chem* **278,** 9142-9149.

Murao, K., V. Terpstra, S. R. Green, N. Kondratenko, D. Steinberg and O. Quehenberger (1997) Characterization of CLA-1, a human homologue of rodent scavenger receptor BI, as a receptor for high density lipoprotein and apoptotic thymocytes. *J Biol Chem* **272,** 17551-17557.

Nakagawa-Toyama, Y., K. Hirano, Tsujii, K., M. Nishida, J. Miyagawa, N. Sakai and S. Yamashita (2005) Human scavenger receptor class B type I is expressed with cell-specific fashion in both initial and terminal site of reverse cholesterol transport. *Atherosclerosis* **183,** 75-83.

Nieland, T. J., M. Ehrlich, M. Krieger and T. Kirchhausen (2005) Endocytosis is not required for the selective lipid uptake mediated by murine SR-BI. *Biochimica et Biophysica Acta* **1734,** 1744-1751.

Nieland, T. J. F., M. Penman, L. Dori, M. Krieger and T. Kirchhausen (2002) Discovery of chemical inhibitors of the selective transfer of lipids mediated by the HDL receptor SR-BI. *Proc Natl Acad Sci U S A* **99,** 15422-15427.

Ohgami, N., R. Nagai, A. Miyazaki, M. Ikemoto, H. Arai, S. Horiuchi and H. Nakayama (2001) Scavenger receptor class B type I-mediated reverse cholesterol transport is inhibited by advanced glycation end products. *J Biol Chem* **276,** 13348-13355.

Pagler, T. A., S. Rhode, A. Neuhofer, H. Laggner, W. Strobl, C. Hinterndorfer, I. Volf, M. Pavelka, E. R. Eckhardt, D. R. van der Westhuyzen, G. J. Schutz and H. Stangl (2006)

SR-BI-mediated high density lipoprotein (HDL) endocytosis leads to HDL resecretion facilitating cholesterol efflux. *J Biol Chem* **281,** 11193-111204.

Parathath, S., M. A. Connelly, R. A. Rieger, S. M. Klein, N. A. Abumrad, M. De La Llera-Moya, C. R. Iden, G. H. Rothblat and D. L. Williams (2004) Changes in plasma membrane properties and phosphatidylcholine subspecies of insect Sf9 cells due to expression of scavenger receptor class B, type I, and CD36. *J Biol Chem* **279,** 41310-41318.

Qiao, J. H., J. Tripathi, N. K. Mishra, Y. Cai, S. Tripathi, X. P. Wang, S. Imes, M. C. Fishbein, S. K. Clinton, P. Libby, A. J. Lusis and T. B. Rajavashisth (1997) Role of macrophage colony-stimulating factor in atherosclerosis: studies of osteopetrotic mice. *Am J Pathol* **150,** 1687-1699.

Reaven, E., Y. Cortez, S. Leers-Sucheta, A. Nomoto and S. Azhar (2004) Dimerization of the scavenger receptor class B type I: formation, function and localization in diverse cells and tissues. *J Lip Res* **45,** 513-528.

Reynolds, G. D. and R. W. St Clair (1985) A comparative and biochemical study of the uptake of fluorescent and 125I-labeled lipoproteins by skin fibroblasts, smooth muscle cells and peritoneal macrophages in culture. *Am J Pathol* **121,** 200-211.

Rhainds, D., P. Bourgeois, G. Bourret, K. Huard, L. Falstrault and L. Brissette (2004) Localization and regulation of SR-BI in membrane rafts of HepG2 cells. *Journal of Cell Science* **117,** 3095-3105.

Rhode, S., A. Breuer, J. Hesse, M. Sonnleitner, T. A. Pagler, M. Doringer, G. J. Schutz and H. Stangl (2004) Visualization of the uptake of individual HDL particles in living cells via the scavenger receptor class B type I. *Cell Biochem Biophys* **41,** 343-356.

Rigotti, A., S. L. Acton and M. Krieger (1995) The class B scavenger receptors SR-BI and CD36 are receptors for anionic phospholipids. *J Biol Chem* **270,** 16221-16224.

Rigotti, A., B. L. Trigatti, M. Penman, H. Rayburn, J. Herz and M. Krieger (1997) A targeted mutation in the murine gene encoding the high density lipoprotein (HDL) receptor scavenger receptor class B type I reveals its key role in HDL metabolism. *Proc Natl Acad Sci U S A* **94,** 12610-12615.

Sahoo, D., Y. F. Darlington, D. Pop, D. L. Williams and M. A. Connelly Scavenger receptor class B type I (SR-BI) assembles into detergent-sensitive dimers and tetramers. (Accepted for publication in Biochimica et Biophysica Acta in March 2006).

Sahoo, D., Y. F. Darlington, D. Pop, D. L. Williams and M. A. Connelly (2006) Scavenger receptor class B type I (SR-BI) assembles into detergent-sensitive dimers and

tetramers. *Biochimica et Biophysica Acta* (Accepted for publication in Biochimica et Biophysica Acta).

Sahoo, D., Y. Peng, J. R. Smith, Y. F. Darlington and M. A. Connelly Scavenger receptor class B, type I (SR-BI) homo-dimerizes via its C-terminal region: Fluorescence resonance energy transfer analysis (Accepted for publication in Biochimica et Biophysica Acta in April 2007).

Sambrook, J. and D. W. Russell. *Molecular Cloning: A Laboratory Manual.* 3rd Edition Cold Spring, New York: Cold Spring Harbor Laboratory Press, 2001.

Seetharam, D., C. Mineo, A. K. Gormley, L. L. Gibson, W. Vongpatanasin, K. L. Chambliss, L. D. Hahner, M. L. Cummings, R. L. Kitchens, Y. L. Marcel, D. J. Rader and P. W. Shaul (2006) High-density lipoprotein promotes endothelial cell migration and reendothelialization via scavenger receptor-B type I. *Circ Res.* **98,** 63-72.

Sehayek, E., R. Wang, J. G. Ono, V. S. Zinchuk, E. M. Duncan, S. Shefer, D. E. Vance, M. Ananthanarayanan, B. T. Chait and J. L. Breslow (2003) Localization of the PE methylation pathway and SR-BI to the canalicular membrane: evidence for apical PC biosynthesis that may promote biliary excretion of phospholipid and cholesterol. *Journal of Lipid Research* **44,** 1605-1613.

Shetty, S., E. R. M. Eckhardt, S. R. Post and D. R. van der Westhuyzen (2006) Phosphatidylinositol-3-kinase regulates scavenger receptor class B type I subcellular localization and selective lipid uptake in hepatocytes *Arterioscler Thromb Vasc Biol* **26,** 2125-2131.

Silver, D. L. (2002) A Carboxyl-terminal PDZ-interacting Domain of Scavenger Receptor B, Type I Is Essential for Cell Surface Expression in Liver. *The Journal of Biological Chemistry* **277,** 34042-34047.

Silver, D. L., N. Wang, X. Xiao and A. R. Tall (2001) High Density Lipoprotein (HDL) Particle Uptake Mediated by Scavenger Receptor Class B Type 1 Results in Selective Sorting of HDL Cholesterol from Protein and Polarized Cholesterol Secretion. *J Biol Chem* **276,** 25287-25293.

Skalen, K., M. Gustafsson, E. K. Rydberg, L. M. Hulten, O. Wiklund, T. L. Innerarity and J. Boren (2002) Subendothelial retention of atherogenic lipoproteins in early atherosclerosis. *Nature* **417,** 750-754.

Stocker, R. and J. F. Keaney, Jr. (2004) Role of oxidative modifications in atherosclerosis. *Physiol Rev* **84,** 1381-1478.

Sun, B., E. R. M. Eckhardt, S. Shetty, D. R. van der Westhuyzen and N. R. Webb (2006) Quantitative analysis of SR-BI-dependent HDL retroendocytosis in hepatocytes and fibroblasts *Journal of Lipid Research* **47,** 1700-1713.

Tall, A. R., X. Jiang, Y. Luo and D. Silver (2000) 1999 George Lyman Duff memorial lecture: lipid transfer proteins, HDL metabolism, and atherogenesis. *Arterioscler Thromb Vasc Biol* **20,** 1185-1188.

Tancevski, I., S. Frank, P. Massoner, U. Stanzl, W. Schgoer, A. Wehinger, C. Fievet, P. Eller, J. R. Patsch and A. Ritsch (2005) Increased plasma levels of LDL cholesterol in rabbits after adenoviral overexpression of human scavenger receptor class B type. *J Mol Med* **83,** 927-932.

Teiger, E. (2001) [Physiopathology of unstable angina]. *Ann Cardiol Angeiol (Paris)* **50,** 359-365.

Tondu, A., C. Robichon, L. Yvan-Charvet, N. Donne, X. Le Liepvre, E. Hajduch, P. Ferré, I. Dugail and G. Dagher (2004) Insulin and angiotensin II induce the translocation of the scavenger receptor class B, type I from intracellular sites to the plasma membrane of adipocytes. *J Biol Chem* **280,** 33536-33540.

Trigatti, B., H. Rayburn, M. Viñals, A. Braun, H. Miettinen, M. Penman, M. Hertz, M. Schrenzel, L. Amigo, A. Rigotti and M. Krieger (1999) Influence of the HDL receptor SR-BI on reproductive and cardiovascular pathophysiology. *Proc Natl Acad Sci U S A* **96,** 9322–9327.

Tulenko, T. N. and A. E. Sumner (2002) The physiology of lipoproteins. *J Nucl Cardiol* **9,** 638-649.

Ueda, Y., E. Gong, L. Royer, P. N. Cooper, O. L. Francone and E. M. Rubin (2000) Relationship between expression levels and atherogenesis in scavenger receptor class B, type I transgenics. *J Biol Chem* **275,** 20368–20373.

Ueda, Y., L. Royer, E. Gong, J. Zhang, P. N. Cooper, O. Francone and E. M. Rubin (1999) Lower plasma levels and accelerated clearance of high density lipoprotein (HDL) and non-HDL cholesterol in scavenger receptor class B type I transgenic mice. *J Biol Chem* **274,** 7165–7171.

Varban, M. L., F. Rinninger, N. Wang, V. Fairchild-Huntress, J. H. Dunmore, Q. Fang, M. L. Gosselin, K. L. Dixon, J. D. Deeds, S. L. Acton, A. R. Tall and D. Huszar (1998) Targeted mutation reveals a central role for SR-BI in hepatic selective uptake of high density lipoprotein cholesterol. *Proc Natl Acad Sci U S A* **95,** 4619–4624.

Viles-Gonzalez, J. F., S. X. Anand, C. Valdiviezo, M. U. Zafar, R. Hutter, J. Sanz, T. Rius, M. Poon, V. Fuster and J. J. Badimon (2004) Update in atherothrombotic disease. *Mt Sinai J Med* **71,** 197-208.

Wang, N., T. Arai, Y. Ji, F. Rinninger and A. R. Tall (1998) Liver-specific overexpression of scavenger receptor BI decreases levels of very low density lipoprotein ApoB, low density lipoprotein ApoB, and high density lipoprotein in transgenic mice. *J Biol Chem* **273,** 32920–32926.

Williams, D. L., M. de La Llera-Moya, S. T. Thuahnai, S. Lund-Katz, M. A. Connelly, S. Azhar, G. M. Anantharamaiah and M. C. Phillips (2000) Binding and cross-linking studies show that scavenger receptor BI interacts with multiple sites in apolipoprotein A-I and identify the class A amphipathic alpha-helix as a recognition motif. *J Biol Chem* **275,** 18897-18904.

Williams, K. J. and I. Tabas (1995) The response-to-retention hypothesis of early atherogenesis. *Arterioscler Thromb Vasc Biol* **15,** 551-561.

Witt, W., I. Kolleck, H. Fechner, P. Sinha and B. Rüstow (2000) Regulation by vitamin E of the scavenger receptor BI in rat liver in HepG2 cells. *J Lip Res* **41,** 2009-2016.

Wüstner, D., M. Mondal, A. Huang and F. R. Maxfield (2004) Different transport routes for high density lipoprotein and its associated free sterol in polarized hepatic cells. *J Lip Res* **45,** 427-437.

Yeh, Y. C., G. Y. Hwang, I. P. Liu and V. C. Yang (2002) Identification and expression of scavenger receptor SR-BI in endothelial cells and smooth muscle cells of rat aorta in vitro and in vivo. *Atherosclerosis* **161,** 95-103.

Yesilaltay, A., O. Kocher, R. Pal, A. Leiva, V. Quinones, A. Rigotti and M. Krieger (2006) PDZK1 is required for maintaining hepatic scavenger receptor, class B, type I (SR-BI) steady state levels but not its surface localization or function. *J Biol Chem* **281,** 28975-28980.

Yuhanna, I. S., Y. Zhu, B. E. Cox, L. D. Hahner, S. Osborne-Lawrence, P. Lu, Y. L. Marcel, R. G. Anderson, M. E. Mendelsohn, H. H. Hobbs and P. W. Shaul (2001) High-density lipoprotein binding to scavenger receptor-BI activates endothelial nitric oxide synthase. *Nat Med* **7,** 853-857.

Zhang, Y., A. M. Ahmed, N. McFarlane, C. Capone, D. R. Boreham, R. Truant, S. A. Igdoura and B. L. Trigatti (2007a) Regulation of SR-BI-mediated selective lipid uptake in Chinese hamster ovary-derived cells by protein kinase signaling pathways. *J Lip Res* **48,** 405-416.

Zhang, Y., A. M. Ahmed, T. Tran, J. Lin, N. McFarlane, D. R. Boreham, S. A. Igdoura, R. Truant and B. L. Trigatti (2007b) The inhibition of endocytosis affects HDL-lipid uptake mediated by the human scavenger receptor class B type I. (Accepted for publication in Molecular Membrane Biology).